To the Graduate Council:

I am submitting herewith a thesis written by Mark A. McBride entitled "Design and Testing of Devices to Prevent Horizontal Tail Stall of the Ball-Bartoe Jetwing Research Aircraft." I have examined the final copy of this thesis for form and content and recommend that it be accepted in partial fulfillment of the requirements for the degree of Master of Science, with a major in Aviation Systems.

Ralph D. Kimberlin, Major Professor

We have read this thesis
and recommend its acceptance:

Accepted for the Council:

Vice Provost
and Dean of the Graduate School

STATEMENT OF PERMISSION TO USE

In presenting this thesis in partial fulfillment of the requirements for a Master's degree at The University of Tennessee, Knoxville, I agree that the Library shall make it available to borrowers under rules of the Library. Brief quotations from this thesis are allowable without special permission, provided that accurate acknowledgment of the source is made.

Permission for extensive quotation from or reproduction of this thesis may be granted by my major professor, or in his absence, by the Head of Interlibrary Services when, in the opinion of either, the proposed use of the material is for scholarly purposes. Any copying or use of the material in this thesis for financial gain shall not be allowed without my written permission.

Signature Mark A McBride

Date August 3, 1989

DESIGN AND TESTING OF DEVICES TO PREVENT HORIZONTAL TAIL STALL OF THE BALL-BARTOE JETWING RESEARCH AIRCRAFT

A Thesis

Presented for the

Master of Science

Degree

The University of Tennessee, Knoxville

Mark A. McBride

December 1989

ACKNOWLEDGMENTS

During the course of my thesis research, a number of persons have generously assisted me. I am especially grateful to Mr. Ralph Kimberlin, who has served as advisor, thesis chairman, and friend. I would also like to thank Dr. J. Wu and Dr. Roger Crawford for serving on my thesis committee and providing me with helpful suggestions during the thesis research.

I am also indebted to Dr. Ahmad Vakili for helping me with the data reduction portion of my research. I would also like to express my sincere thanks to the employees of the Gas Dynamics and Flight Research Divisions of the University of Tennessee Space Institute for their help during this project.

ABSTRACT

Since its inception, the Ball-Bartoe Jetwing Research Aircraft has been plagued with the problems of horizontal tail stall and static longitudinal instability. The tail stall problem is primarily due to the large downwash at the tail due to the Jetwing's Upper Surface Blowing concept of propulsive lift, and due to the thin, symmetric NACA 0008 airfoil section used for the aircraft's horizontal tail. These characteristics also contribute to the instability of the Jetwing, as do the aircraft's center of gravity and low tail volume coefficient.

Several possible aircraft modifications were examined to determine if they alleviated the tail stall and stability problems. The two most promising modifications, a leading-edge slat and a leading-edge droop device, were tested on a quarter-scale half span model of the Jetwing horizontal tail in the University of Tennessee Space Institute's Low-Speed Wind-Tunnel. The results of these tests show that while both the slat and droop configurations improve the Jetwing's horizontal tail stall capabilities, neither modification affected the aircraft's stability problem significantly.

TABLE OF CONTENTS

CHAPTER		PAGE
I.	INTRODUCTION	1
II.	DESCRIPTION OF BALL-BARTOE JETWING	3
III.	DEFINITION OF PROBLEMS OF JETWING	9
	Horizontal Tail Stall	9
	Static Longitudinal Instability	15
	The Need for Solutions	22
IV.	DISCUSSION OF POSSIBLE SOLUTIONS	23
	Introduction	23
	Center of Gravity Shift	24
	Movement of Horizontal Tail	25
	Redesign of Horizontal Tail	25
	Boundary Layer Control	26
	Addition of a Leading-Edge Slat	27
	Addition of Leading-Edge Droop	32
V.	WIND-TUNNEL TESTS OF PROPOSED MODIFICATIONS	35
	Introduction	35
	Description of the Test Model	35
	Test Procedure	36
VI.	RESULTS AND DISCUSSION	39
	Horizontal Tail Stall	39
	Static Longitudinal Stability	70
VII.	CONCLUSIONS AND RECOMMENDATIONS	74

CHAPTER

PAGE

BIBLIOGRAPHY 77

VITA 79

LIST OF FIGURES

FIGURES		PAGE
1.	Upper Surface Blowing Concept [3]	4
2.	Ball-Bartoe Jetwing Upper Surface Blown Aircraft [2]	8
3.	The NACA 0008 Airfoil and Its Coordinates [4]	11
4.	NACA 0008 Lift Coefficient Versus Angle of Attack [4]	12
5.	Flow Angles of the Ball-Bartoe Jetwing [2]	13
6.	Forces Acting on an Aircraft in Flight	16
7.	Wing Lift-Curve Slope versus Blowing Coefficient for Various Flap Deflections	19
8.	Wing Leading-Edge and Horizontal Tail Leading-Edge Slats	28
9.	Sisterman's Proposed Thin Slat Design at the Maximum Chord Position [4]	30
10.	Planform View of the Horizontal Tail with the Proposed Modification of the Sisterman Slat [14]	31
11.	Proposed Leading-Edge Droop Modificaiton for Jetwing Horizontal Tail	34
12.	Quarter-Scale Model of Jetwing Half-Tail	37
13.	Flow Visualization of Jetwing Horizontal Tail Model with No Modifications and 0-Degree Elevator Deflection . .	40

FIGURES PAGE

14. Flow Visualization of Jetwing Horizontal Tail Model with No Modifications and 10-Degree Elevator Deflection 42

15. Flow Visualization of Jetwing Horizontal Tail Model with No Modifications and 20-Degree Elevator Deflection 44

16. Flow Visualization of Jetwing Horizontal Tail Model and 30-Degree Elevator Deflection 46

17. Flow Visualization of Jetwing Horizontal Tail Model with Leading-Edge Slat and 0-Degree Elevator Deflection 48

18. Flow Visualization of Jetwing Horizontal Tail Model with Leading-Edge Slat and 10-Degree Elevator Deflection 50

19. Flow Visualization of Jetwing Horizontal Tail Model with Leading-Edge Slat and 20-Degree Elevator Deflection 52

20. Flow Visualization of Jetwing Horizontal Tail Model with Leading-Edge Slat and 30-Degree Elevator Deflection 54

21. Flow Visualization of Jetwing Horizontal Tail Model with Leading-Edge Droop and 0-Degree Elevator Deflection 56

FIGURES PAGE

22. Flow Visualization of Jetwing Horizontal Tail Model with Leading-Edge Droop and 10-Degree Elevator Deflection 58

23. Flow Visualization of Jetwing Horizontal Tail Model with Leading-Edge Droop and 20-Degree Elevator Deflection 60

24. Flow Visualization of Jetwing Horizontal Tail Model with Leading-Edge Droop and 30-Degree Elevator Deflection 62

25. Lift Coefficient versus Angle of Attack for Plain Model 64

26. Lift Coefficient versus Angle of Attack for Leading-Edge Slat Modification 65

27. Lift Coefficient versus Angle of Attack for Leading-Edge Droop Modification 66

28. Characteristic Drag Polar for All Test Models 67

LIST OF TABLES

TABLE		PAGE
1.	Jetwing Physical Description [1]	5
2.	Performance Characteristics of the Ball-Bartoe Jetwing [3]	7
3.	Solies' Experimental Determination of Flow Angles of the Ball-Bartoe Jetwing [2]	14
4.	Horizontal Tail Volume Coefficient Comparison of Powered-Lift Aircraft [1]	21
5.	Test Matrix of Jetwing Tail Model	38
6.	Summary of Flow Visualization Tests	71
7.	Horizontal Tail Volume Coefficient Comparison of Proposed Modifications	73

LIST OF SYMBOLS AND ABBREVIATIONS

Latin Symbols

A	Aspect ratio
$a_{o,t}$	Horizontal tail section lift-curve slope
a_t	Horizontal tail lift-curve slope
a_w	Wing lift-curve slope
b	Wing span
C_D	Drag coefficient = drag/qS
C_J	Blowing coefficient = thrust/qS
$C_{J(s)}$	Stabilized blowing coefficient
$C'_{J(s)}$	Corrected stabilized blowing coefficient
C_L	Lift coefficient = lift/qS
C_{L_T}	Horizontal tail lift coefficient
C_m	Moment coefficient = moment/qSb
D	Drag
F_G	Gross thrust
h	Center of gravity location
i_T	Horizontal tail incidence angle
L	Lift
L_T	Horizontal tail lift
ℓ_T	Distance from aerodynamic center tail to center of gravity
M	Moment
N_I	Inlet force
$N1$	Maximum engine rotor speed

q	Dynamic pressure = $1/2\ \rho V^2$
S_T	Horizontal tail area
S_w	Wing area
S'	Blown area on wing
V	Airspeed
V_H	Horizontal tail volume coefficient
X_a	Distance from wing aerodynamic center to center of gravity

Greek Symbols

α	Wing angle of attack
$\alpha_{(s)}$	Stabilized wing angle of attack
α_T	Horizontal tail angle of attack
$\delta_{(s)}$	Stabilized blowing deflection
δ_F	Wing flap deflection
ε	Downwash angle
ε_T	Downwash angle at horizontal tail
ΣM_{cg}	Sum of moments about aircraft center of gravity
η_T	Horizontal tail dynamic efficiency
ρ	Air density
$\xi\alpha_{(s)'}$	Stabilized aerodynamic center due to angle of attack
$\xi\alpha_{(s)}$	Stabilized aerodynamic center due to blowing

Abbreviations

A/C	Aircraft

a.c.	Aerodynamic center
c.g.	Center of gravity
deg	Degrees
Elev	Elevator deflection
ft	Feet
Fuse	Fuselage
in	Inlet
in.	Inches
kts	Knots
L.E.	Leading edge
MAC	Mean Aerodynamic Chord
max	Maximum
min	Minimum
QSRA	Quiet Short-Haul Research Aircraft
STOL	Short Takeoff and Landing
USB	Upper Surface Blowing
UTSI	University of Tennessee Space Institute

CHAPTER I

INTRODUCTION

The purpose of this thesis is to investigate possible solutions to the problems of horizontal tail stall and static longitudinal instability of the Ball-Bartoe Jetwing research aircraft. The Jetwing is a Short Takeoff and Landing (STOL) aircraft that uses an Upper Surface Blowing (USB) concept to achieve STOL characteristics. The aircraft is presently owned and operated by the University of Tennessee Space Institute.

The primary reason for the aforementioned problems of the Jetwing is the airflow characteristics about the horizontal tail of the aircraft [1][1]. Because the nature of Upper Surface Blowing results in a large amount of downwash directed from the aircraft's wing, a large effective angle of attack at the horizontal tail is generated. Consequently, the NACA 0008 symmetric airfoil that is used for the Jetwing's horizontal tail is subject to stalling. In addition, the large amount of downwash (due to USB) and the low lift-curve slope of the NACA 0008 airfoil adversely affects the Jetwing's horizontal tail contribution to static longitudinal stability. In addition, the aft center of gravity location of the aircraft also diminishes the horizontal tail's contribution to aircraft static longitudinal stability.

---

[1]Numbers in brackets refer to similarly numbered references in the Bibliography.

This thesis will examine many potential solutions to these problems. Each solution will be examined to determine if it meets the basic constraints of weight, cost and overall simplicity. In addition, each potential solution will be examined to ascertain if it solves both the problems of horizontal tail stall and static longitudinal instability.

The physical characteristics of the Ball-Bartoe Jetwing are covered in Chapter II, while the causes of the problems of tail stall and longitudinal instability are discussed in Chapter III. Possible solutions and testing of proposed solutions are shown in Chapters IV and V. The results and conclusions derived from tests are given in Chapters VI and VII.

CHAPTER II

DESCRIPTION OF BALL-BARTOE JETWING

The Ball-Bartoe Jetwing is a Short Takeoff and Landing (STOL), technology demonstrator aircraft designed and manufactured by the Ball Aircraft Corporation of Colorado in 1976. After numerous flight tests by the Ball Corporation, the aircraft and its accompanying patents were donated to the University of Tennessee Space Institute, where it now resides. Prior to this donation, the aircraft underwent extensive wind-tunnel testing at the National Aeronautic and Space Administration Ames Research Laboratory [1,2].

The Ball-Bartoe Jetwing uses the concept of Upper Surface Blowing (USB) to achieve powered lift-STOL capabilities. The Pratt and Whitney JT15D-1 turbofan engine's exhaust is directed over 70 percent of the aircraft's wing span. A single element Coanda flap is located at the trailing edge of the wing to help maintain attached flow over the wing's trailing edge [1]. Figure 1 depicts the Upper Surface Blowing concept used on the Ball-Bartoe Jetwing [2].

A basic physical description of the Jetwing is given in Table 1 [1]. Basic performance characteristics of the Jetwing are given in Table 2 [3]. Figures of the aircraft are shown in Figure 2 [2].

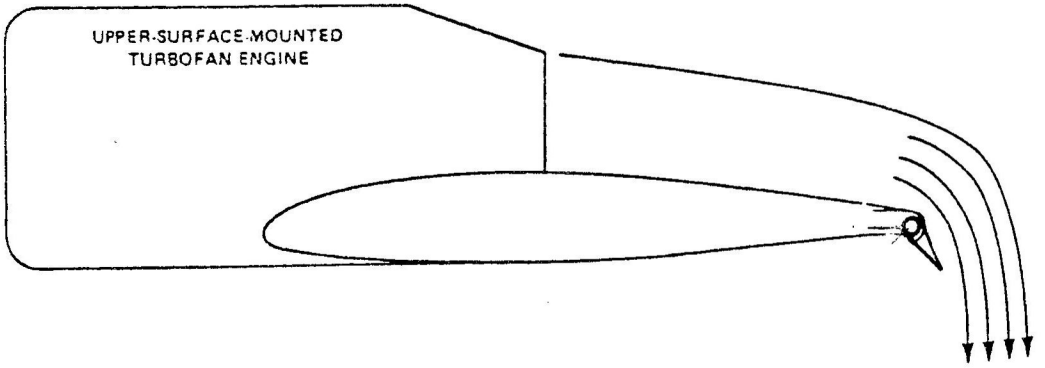


Figure 1. Upper Surface Blowing Concept [3]

Table 1. Jetwing Physical Description [1]

Aircraft Parameter	Description
Power Plant	Pratt & Whitney JT15D-1 Turbofan
Fuel Capacity	106 gallons
Maximum Takeoff Gross Weight	3750 pounds
Empty Weight	2742 pounds (with ballast)
Ballast	412 pounds
Center of Gravity (with ballast, fuel, and pilot)	35.5% MAC
Wing Airfoil Section	NACA 23020 Modified at Root NACA 23015 at Tip
Wing Span	21.75 ft
Wing Area	105.6 ft^2
Wing Aspect Ratio	4.48
Wing Mean Aerodynamic Chord	5.08 ft
Taper Ratio	0.46
Wing Incidence	0° Root; 0° Tip
Aileron Type	Setback Hinge
Aileron Span	35.75 in. each
Aileron Area	6.88 ft^2 total
Aileron Deflection	±25°
Flap Type	Coanda Single Element
Flap Span	69 in. each
Flap Area	21.2 ft^2 Total
Flap Deflection	0° to 55°

Table 1. Concluded

Aircraft Parameter	Description
Horizontal Tail Airfoil Section	NACA 0008
Horizontal Tail Span	9.33 ft
Horizontal Tail Area	27.5 ft^2
Horizontal Tail Aspect Ratio	3.16
Horizontal Tail Volume Coefficient (V_H)	0.74
Elevator Type	Shielded Horn
Elevator Area	13.25 ft^2
Elevator Deflection	+29° to -25°
Horizontal Stabilizer Trim Deflection	+20° to -2°
Vertical Tail Airfoil Section	8% Thick Symmetrical
Vertical Tail Span	5.67 ft
Vertical Tail Area	18.33 ft^2
Vertical Tail Aspect Ratio	1.75
Vertical Tail Volume Coefficient (V_V)	0.115
Rudder Area	8.06 ft^2
Rudder Deflection	±20°
Aircraft Length	28.6 ft
Aircraft Height	6.1 ft

Table 2. Performance Characteristics of the Ball-Bartoe Jetwing [3]

Performance Parameter	Value
Maximum Level Flight Speed	347 kt
Minimum Control Speed	35 kt
Landing Speed	60 kt
Takeoff Distance (with 50 ft Obstacle)	1250 ft
Landing Run at Sea Level	700-800 ft
Rate of Climb at Sea Level	6,000 ft/min

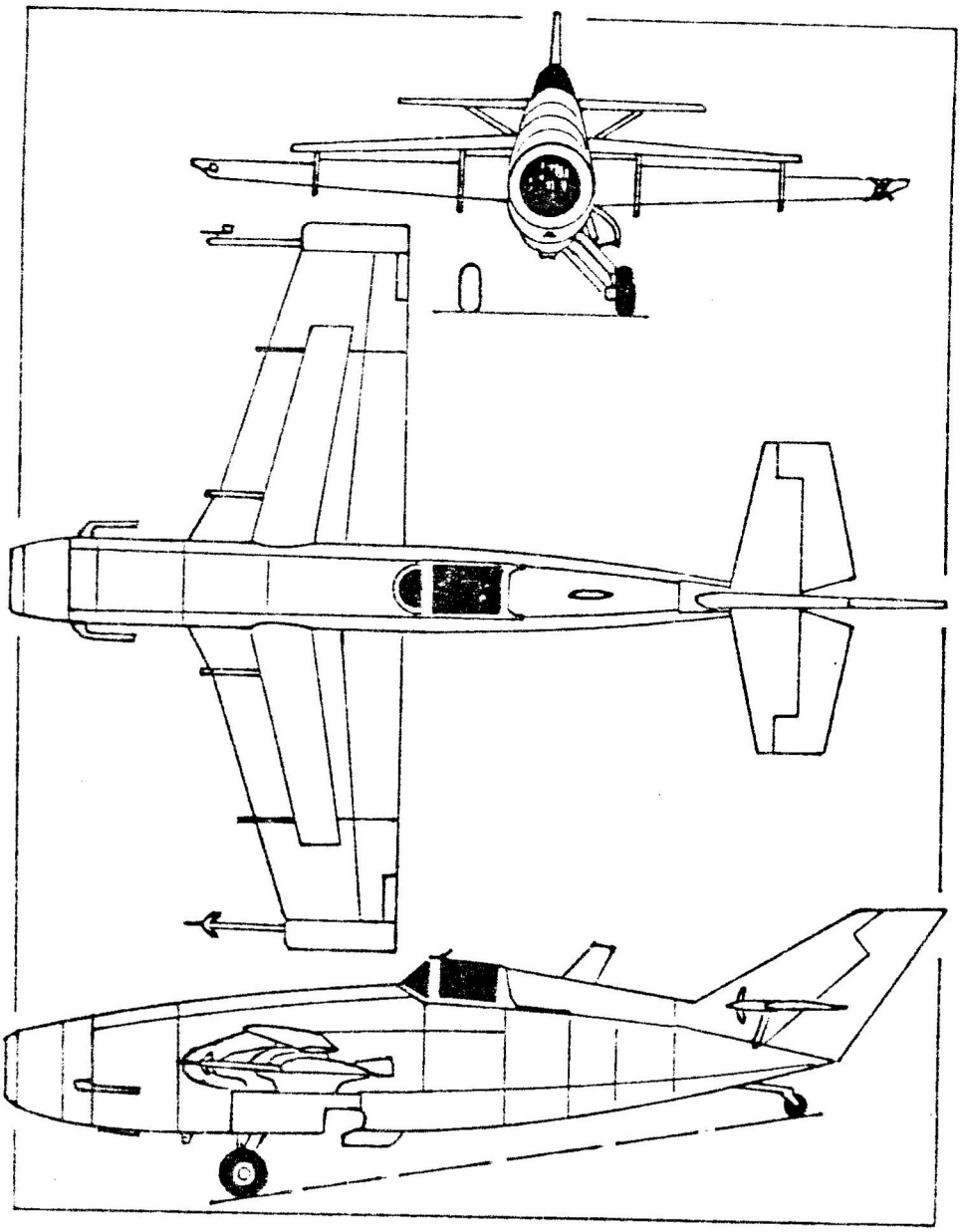


Figure 2. Ball-Bartoe Jetwing Upper Surface Blown Aircraft [2]

CHAPTER III

DEFINITION OF PROBLEMS OF JETWING

Horizontal Tail Stall

During flight tests of the Ball-Bartoe Jetwing by the Ball Aircraft Corporation, the aircraft's horizontal tail stalled at a indicated airspeed of 50 knots and a flap deflection of 45 degrees. After noticing this phenomenon, the Ball test team limited the Jetwing's flap extension to 35 degrees [3].

In addition, during an extensive flight test program for the United States Navy (performed by the University of Tennessee Space Institute), a partial horizontal tail stall occurred at a calibrated airspeed of 52 knots and a 30 degree flap deflection. During this tail stall, the power setting of the aircraft's engine was approximately 90% of the engine maximum rotor speed (N_1), and the landing gear was locked in a down position [1].

The reasons for the horizontal tail stall of the Jetwing are twofold; both the high degree of downwash at the tail and the thin, symmetric airfoil section used for the horizontal tail contribute to this problem. Due to the nature of the USB concept, a large amount of jet exhaust and airflow over the wing is directed downward by the wing's trailing-edge Coanada flap. This situation creates a large downwash angle, ε_t, at the horizontal tail of the aircraft, which in

turn causes a large effective tail angle of attack, α_t. This tail angle of attack can be mathematically defined as [2]:

$$\alpha_T = \alpha + i_T - \varepsilon_T \tag{1}$$

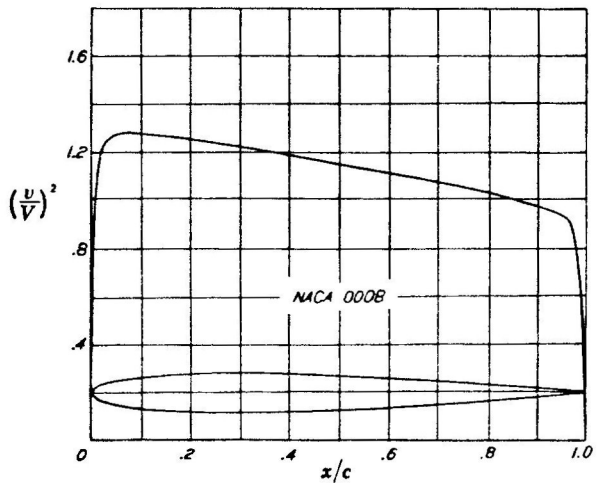
where: α = wing angle of attack

i_T = tail incidence angle

ε_T = horizontal tail downwash angle

Therefore, as the downwash term is increased (due to large flap deflections and USB effects), the tail angle of attack becomes increasingly negative. Because the thin NACA 0008 airfoil section that is used for the aircraft's horizontal tail stalls at a relatively low angle of attack, the Jetwing is certain to encounter horizontal tail stall under the conditions mentioned above. Figure 3 depicts the NACA airfoil and its coordinates; Figure 4 shows the plot of lift coefficient versus angle of attack (C_L vs α) for the NACA 0008 airfoil section [4]. Figure 5 shows the flow characteristics about a USB aircraft's wing and horizontal tail [2].

Solies [2] has conducted research on the airflow characteristics about the horizontal tail of the Ball-Bartoe Jetwing. Results of Solies' research, including major flow angles about the wing and horizontal tail of the Jetwing, airspeeds, and power settings (for various flight test conditions) are shown in Table 3. While the results from Solies' research are quite limited, these are the only results known to the author that include airflow characteristics about the horizontal tail of the aircraft.



x (per cent c)	y (per cent c)	$(v/V)^2$	v/V	$\Delta r_a/V$
0	0	0	0	2.900
0.5	.....	0.792	0.890	1.795
1.25	1.263	1.103	1.050	1.310
2.5	1.743	1.221	1.105	0.971
5.0	2.369	1.272	1.128	0.694
7.5	2.800	1.284	1.133	0.561
10	3.121	1.277	1.130	0.479
15	3.564	1.272	1.128	0.379
20	3.825	1.259	1.122	0.318
25	3.961	1.241	1.114	0.273
30	4.001	1.223	1.106	0.239
40	3.869	1.186	1.089	0.188
50	3.529	1.149	1.072	0.152
60	3.043	1.111	1.054	0.121
70	2.443	1.080	1.039	0.096
80	1.749	1.034	1.017	0.071
90	0.965	0.968	0.984	0.047
95	0.537	0.939	0.969	0.031
100	0.084	.....	.....	0

L.E. radius: 0.70 per cent c

Figure 3. The NACA 0008 Airfoil and Its Coordinates [4]

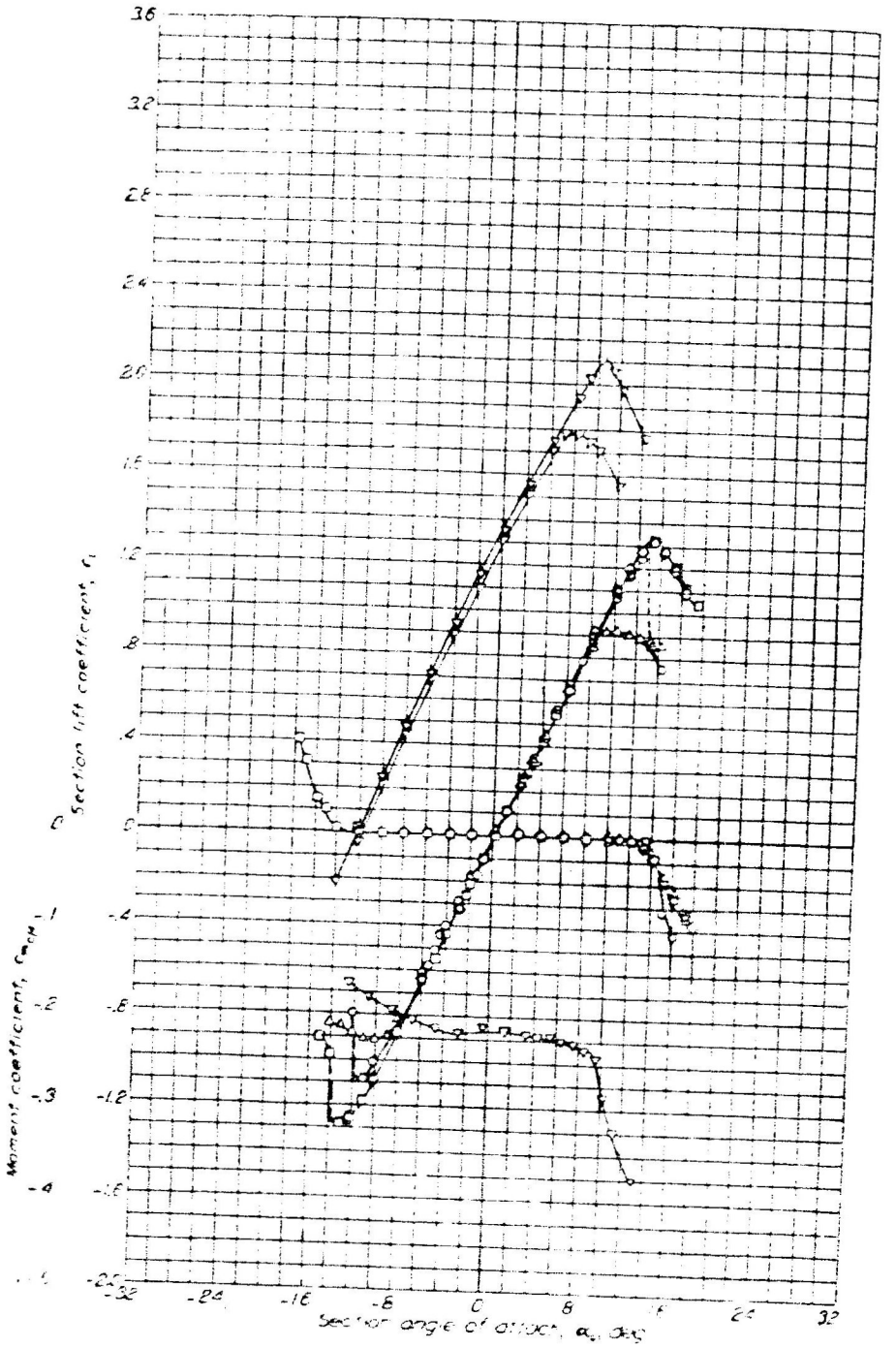


Figure 4. NACA 0008 Lift Coefficient Versus Angle of Attack [4]

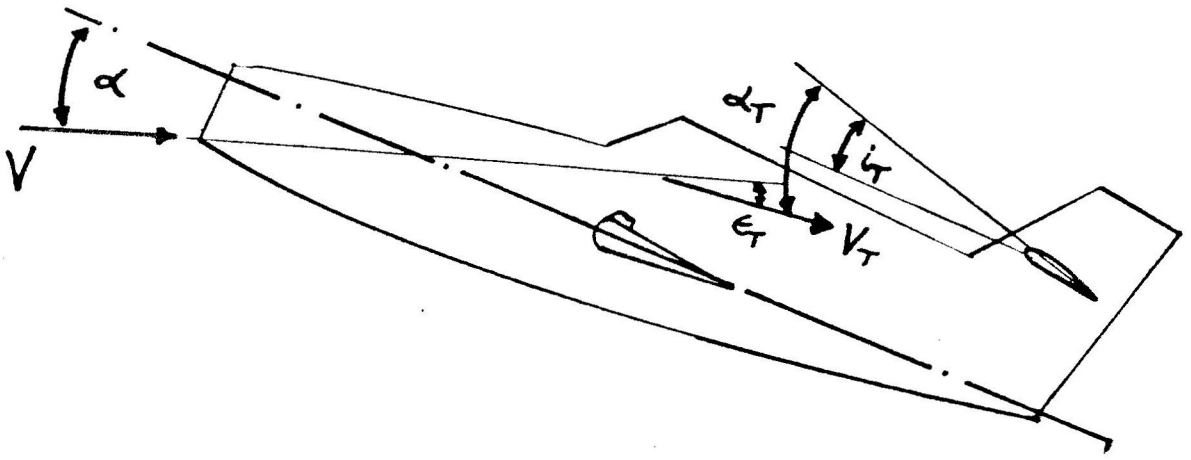


Figure 5. Flow Angles of the Ball-Bartoe Jetwing [2]

Table 3. Solies' Experimental Determination of Flow Angles of the Ball-Bartoe Jetwing [2]

No.	Flaps (deg)	True Airspeed (kts)	Elev. (deg)	C_J	α (deg)	i_T (deg)	ε_T (deg)	α_T (deg)
1	15	108.9	-1.5	0.25	4.5	4.9	8.1	1.3
2	15	87.7	-1.0	0.36	10.0	5.9	12.0	3.9
3	15	77.7	-0.5	0.53	12.0	4.1	13.8	2.3
4	15	67.1	-0.5	0.72	18.0	2.6	12.8	2.8
5	15	78.1	-2.0	0.49	12.5	4.1	2.6	4.0
6	15	89.1	-2.0	0.38	9.0	3.2	9.8	2.4
7	30	91.4	0.0	0.42	2.0	7.4	14.8	-5.4
8	30	76.3	0.0	0.58	5.0	5.6	15.9	-5.3
9	0	104.7	-4.0	0.17	9.5	5.4	5.6	9.3
10	0	93.7	-4.2	0.20	11.5	6.3	2.5	10.3
11	0	85.1	-3.2	0.35	14.0	13.1	15.3	11.8
12	0	76.5	-4.0	0.43	18.2	12.8	20.0	11.0
13	30	64.5	0.7	0.94	12.0	13.4	24.0	6.4
14	30	97.8	0.7	0.37	1.0	7.5	12.5	-4.0
15	45	76.7	1.2	0.69	-1.0	7.7	20.9	-14.2
16	45	64.4	2.0	0.96	4.2	-3.5	25.3	-24.6

Static Longitudinal Instability

During flight tests by the Ball Aircraft Corporation and the University of Tennessee Space Institute, flight test engineers learned that the Jetwing was statically, longitudinally unstable in the climb and powered approach flight regimes [1]. Kimberlin [1] noted that there are four primary reasons for this problem: the extreme aft location of the aircraft's center of gravity, the high degree of downwash created by USB effects, the low lift-curve slope of the aircraft's horizontal tail, and the aircraft's small horizontal tail volume coefficient.

Static longitudinal stability may be defined as the tendency of an aircraft to return to a trimmed condition after it has been displaced from its original trimmed condition [5]. By summing the moments of Figure 6 about the aircraft's center of gravity, an aircraft in stable (trimmed) flight may be mathematically expressed as:

$$\Sigma M_{cg} = 0 \tag{2}$$

In nondimensional terms, static longitudinal stability may be defined as:

$$\left(\frac{dC_m}{dC_L} \right)_{A/C} < 0 \tag{3}$$

By summing the moments in Figure 6, and nondimensionalizing these moments, Equation (3) may be rewritten as [6]:

$$0 > \frac{X_a}{\bar{c}} \left(\frac{dC_m}{dC_L} \right)_{fuse} + \left(\frac{dC_m}{dC_L} \right)_{in} - \left(\frac{a_t}{a_w} \right) V_H \eta_T (1 - d\varepsilon/d\alpha) \tag{4}$$

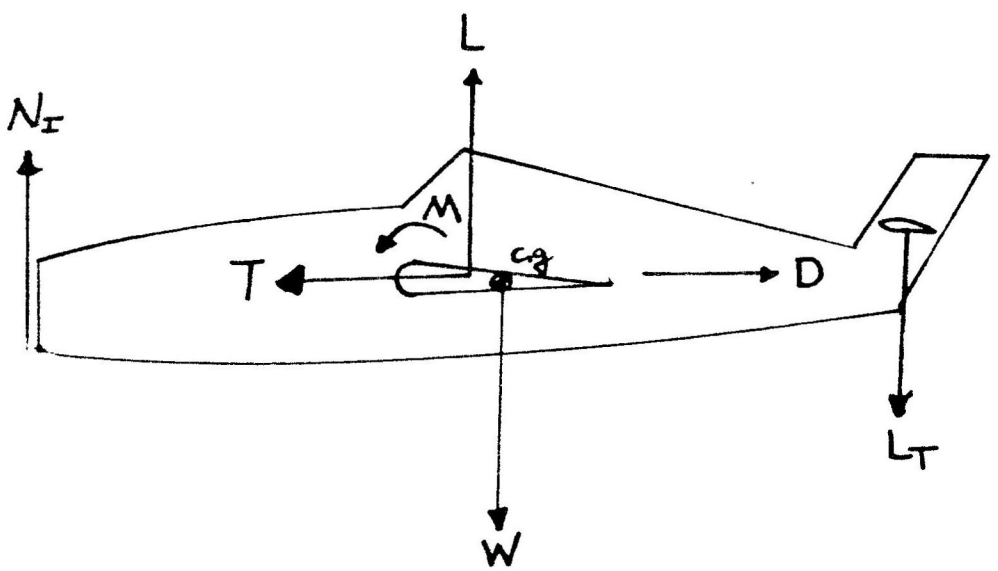


Figure 6. Forces Acting on an Aircraft in Flight

where: X_a = distance between aircraft's center of gravity and the wing aerodynamic center

$\bar{c}$ = mean aerodynamic chord of the wing

a_t = tail lift-curve slope

a_w = wing lift-curve slope

$(dC_m/dC_L)_{fuse}$ = fuselage term of stability

$(dC_m/dC_L)_{in}$ = engine inlet term of stability

V_H = horizontal tail volume coefficient

η_T = tail dynamic efficiency

$d\varepsilon/d\alpha$ = downwash angle change per angle of attack change

One can see from Figure 6 that an aircraft's static longitudinal stability is greatly dependent upon the position of the aircraft's center of gravity. In order to maintain satisfactory static longitudinal stability, most aircraft are designed so that their center of gravity travel is between approximately 20 to 35 percent of the aircraft's mean aerodynamic chord (MAC) [7]. From Table 1, page 5, the Jetwing's center of gravity (for a fully loaded condition) is at 35.5% MAC [1]. Thus, it is difficult to fly the Jetwing in a statically stable longitudinal mode.

The horizontal tail of the Ball-Bartoe Jetwing also contributes to the aircraft's static longitudinal stability problems. The tail's contribution to overall static longitudinal stability can be expressed as [6]:

$$\left(\frac{dC_m}{dC_L}\right)_{tail} = \frac{-a_t}{a_w}(V_H)\eta_T\left(1 - \frac{d\varepsilon}{d\alpha}\right) \qquad (5)$$

Because the change in downwash angle per angle of attack change approaches one (due to USB effects), the horizontal tail's contribution to overall stability approaches zero. Kimberlin [8] has derived a method for predicting the downwash term in Equation (5). The downwash derivative may be defined as:

$$\frac{d\varepsilon}{d\alpha} = \frac{2a_w}{\pi A} \tag{6}$$

where: A = wing aspect ratio

a_w = wing lift-curve slope in 1/rad

The Jetwing's aspect ratio is fixed at 4.48. However, the wing's lift-curve slope, a_w, is a function of both blowing coefficient and flap deflection. The aircraft blowing coefficient, C_J, may be defined as:

$$C_J = \frac{F_G}{qS} \tag{7}$$

where: F_G = aircraft gross thrust in lb

q = dynamic pressure in lb/ft^2

S = wing area in ft^2

The author has generated a plot of blowing coefficient versus wing lift-curve slope (for various flap deflections), for the Jetwing, based upon NASA Ames wind tunnel results for lift-curve slope, blowing coefficient, and flap deflection [9]. This plot can be found in Figure 7.

The low lift-curve slope of the tail, a_t, also diminishes the Jetwing's horizontal tail contribution to static longitudinal stability.

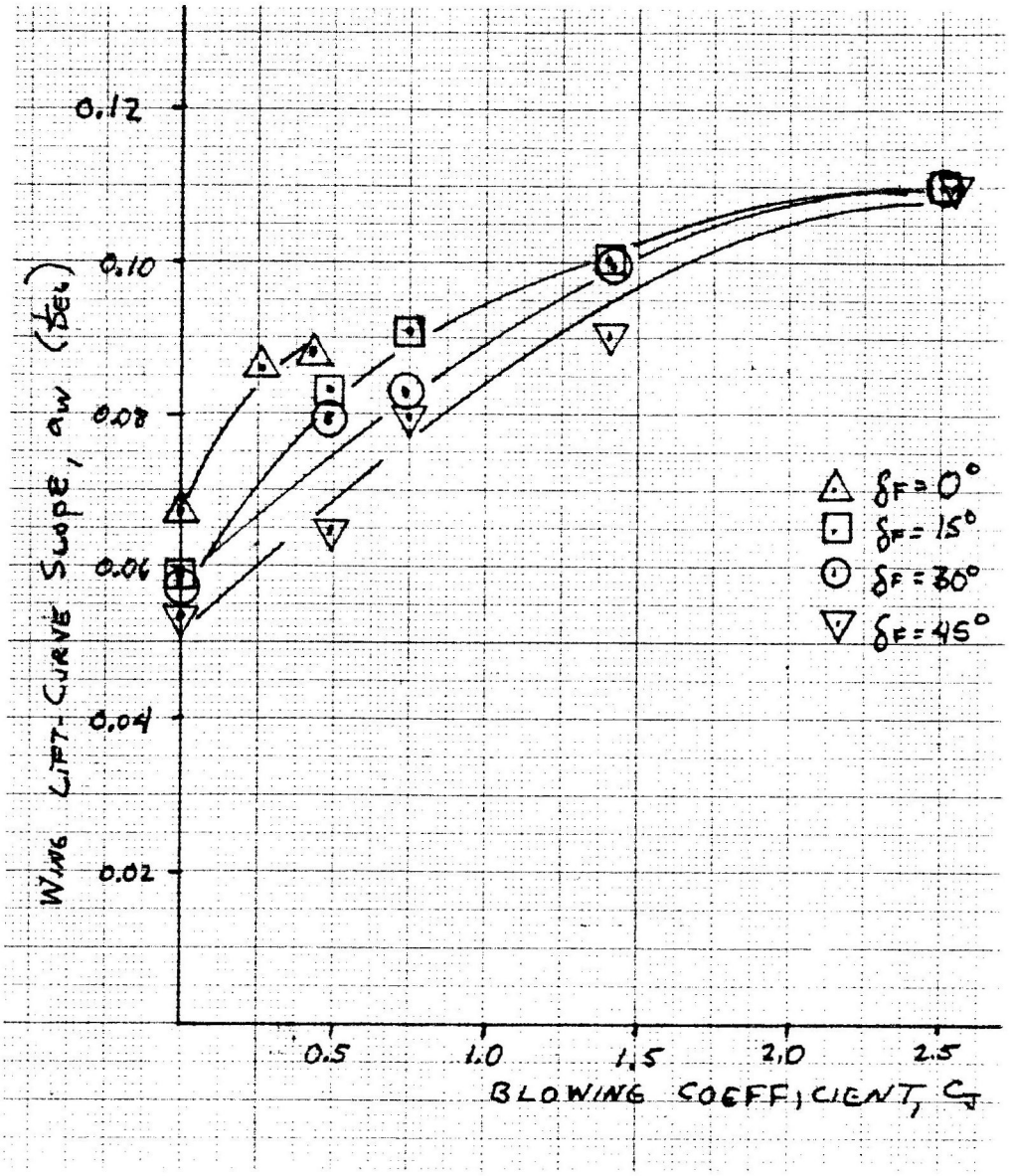


Figure 7. Wing Lift-Curve Slope versus Blowing Coefficient for Various Flap Deflections [9]

stability. The NACA 0008 airfoil section's lift curve slope is 0.109 per degree. Using McCormick's formula for translating section lift-curve slope to that of a three-dimensional lifting surface [5]:

$$a_t = a_{o,t}\left[\frac{A}{A + 2(A+4)/(A+2)}\right] \tag{8}$$

where: $a_{o,t}$ = tail section lift-curve slope

A = lifting surface aspect ratio

the horizontal tail's lift curve slope becomes 0.058 per degree. This value appears to be quite low, and thus is a detriment to the Jetwing's horizontal tail contribution to static longitudinal stability.

In addition, the low value of the Jetwing's horizontal tail volume coefficient diminishes its contribution to stability. The horizontal tail volume coefficient is defined as [7]:

$$V_H = \left[\frac{\ell_T S_T}{\bar{c}\, S_w}\right] \tag{9}$$

where: ℓ_T = distance from tail a.c. to aircraft c.g.

S_T = horizontal tail surface area

$\bar{c}$ = wing mean aerodynamic chord

S_W = wing surface area

When one compares the Jetwing's horizontal tail volume coefficient with those of other aircraft using a powered-lift concept (Table 4), it is evident that the small tail volume coefficient also adversely affects

Table 4. Horizontal Tail Volume Coefficient Comparison of Powered-Lift Aircraft [1]

Aircraft	Horizontal Tail Volume Coefficient, V_H
Jetwing JW-1	0.74
YC-15	1.323
YC-14	1.60
NASA QSRA	1.898

the Jetwing's horizontal tail contribution to static longitudinal stability [1].

The Need for Solutions

Because of the horizontal tail stall problems, the aircraft cannot operate at high flap deflections. Therefore, takeoff and landing performance are degraded due to the fact that the aircraft cannot produce as much lift (for takeoff) or drag (for landing) as desired. The tail stall and static longitudinal instability of the Jetwing also increase pilot workload, as he is forced to hold the aircraft in position (trim control is difficult).

In addition, Federal Air Regulations prohibit a civilian aircraft from normal operations when it is statically longitudinally unstable [10]. Thus, before the Jetwing can become a certified civilian aircraft (other than in experimental category) aircraft, it must exhibit acceptable static longitudinal stability. It is apparent then that solutions to the problems of the Jetwing need to be generated.

CHAPTER IV

DISCUSSION OF POSSIBLE SOLUTIONS

Introduction

While there may be a multitude of possible design solutions to the Ball-Bartoe Jetwing's problems of horizontal tail stall and static longitudinal instability, certain constraints for any possible design solution must be met. Therefore, any discussion of possible solutions must meet the constraints of weight, drag, cost, and design simplicity. In addition, it is necessary for any solution to solve both of the problems of the Jetwing.

Because the Jetwing's center of gravity is farther aft than that of most conventional aircraft, any modifications that impose additional weight to the aircraft - especially when applied behind the center of gravity - must be closely examined. Therefore, any aircraft modification (as a design solution) to the Jetwing must be as light as possible.

In addition, any modifications to the Ball-Bartoe Jetwing that are inexpensive would be most advantageous. Because the Jetwing is a technology demonstrator aircraft, and not a production model, expensive modifications to the aircraft would not be justifiable; it would be more advantageous to rebuild the entire aircraft, with changes incorporated into the new design. Therefore, any design solution should be as inexpensive as possible.

Such solutions should also be simple in design and construction. Complex modifications to the aircraft would almost certainly result in large weight increases. In addition, while a complex solution may solve the problems of tail stall and instability of the aircraft, it may result in additional problems (such as structural difficulties). Therefore, design solutions that involve complex modifications to the aircraft should be avoided.

Design modifications to the Jetwing also need to be drag efficient. If a large drag change is introduced to the aircraft, performance characteristics of the Jetwing will be degraded. The aircraft was designed with certain drag assumptions; in terms of operational capabilities, drastic drag changes would result in a different type of aircraft.

Center of Gravity Shift

As mentioned before, the Ball-Bartoe Jetwing's center of gravity is more aft than that of most aircraft using a conventional horizontal tail configuration. This characteristic is a large contribution to the aircraft's inherent static longitudinal stability problems. Therefore, moving the aircraft's center of gravity forward would certainly benefit the aircraft's stability characteristics.

However, as noted in Table 1, page 5, ballast weight totaling 412 pounds has already been added to the nose of the Jetwing in order to

shift the aircraft's center of gravity forward [1]. Therefore, any further forward center of gravity shift is unlikely.

In addition, while a forward center of gravity shift would certainly enhance the aircraft's static longitudinal stability, it would adversely affect the horizontal tail stall situation. Therefore, the possibility of attempting to move the Jetwing's center of gravity forward is not a viable solution to the problems of the aircraft.

Movement of Horizontal Tail

As mentioned before, a large contribution to the tail stall and instability problems of the Jetwing arise from the large downwash at the tail of the aircraft due to Upper Surface Blowing. Therefore, if the horizontal tail were moved such that it would be free from the wing's downwash, both of these problems would be alleviated. Kimberlin [1] noted this possibility and remarked that future aircraft using the USB concept should employ a canard or t-tail configuration.

However, moving the horizontal tail of the Ball-Bartoe Jetwing would require major structural changes and would undoubtedly involve major expense. Therefore, movement of the horizontal tail is not a viable solution when examined for the constraint of structural simplicity.

Redesign of Horizontal Tail

Another possible solution to the stability and tail stall problems of the Jetwing would be to redesign the aircraft's horizontal tail

airfoil section. Kimberlin [1] noted this possibility, stating that a new airfoil section utilizing more camber and a larger leading edge radius would possibly alleviate the Jetwing's problems.

However, wind-tunnel studies on horizontal tail surfaces, conducted by Harper [11], for various airfoil sections using a horn balanced elevator (such as that employed on the Jetwing) and small aspect ratios (from 3.0 to 3.5), showed that the horizontal tail's airfoil section affected its lift-curve slope very little. This observation is confirmed by Nicolai [7] for low aspect ratio lifting surfaces.

Redesigning the horizontal tail of the Jetwing would also require much structural rework, and thus weight, at the rear of the aircraft. Therefore, major redesign of the horizontal tail is not a viable solution to the problems of the Jetwing.

Boundary Layer Control

Another possible solution to the problems of the Jetwing's horizontal tail is to use some form of laminar flow control on the horizontal tail of the aircraft. By blowing or sucking the boundary layer of the horizontal tail, airflow separation, and thus stalling effects, could possibly be prevented. However, designing a device that artificially introduces flow control to the aircraft's horizontal tail would require a major redesign of the tail's internal structure and would add weight to the tail of the aircraft. Therefore, the possibility of artificial flow control is not a feasible solution to the problems of the Jetwing.

Addition of a Leading-Edge Slat

As mentioned before, a large reason for the Jetwing's stability and tail stall problems is the NACA 0008 airfoil section used for the horizontal tail of the aircraft. Both a low lift-curve slope and low stall angle are characteristic of the NACA 0008 airfoil. Therefore, any modification to the horizontal tail that would increase both its surface area and stall angle would be beneficial. One such modification is the addition of a leading-edge slat.

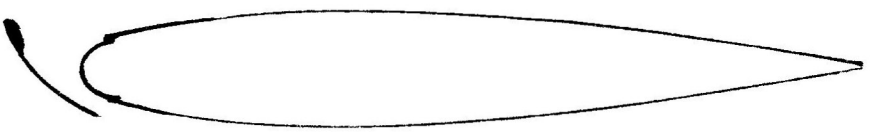
A leading-edge slat is basically an auxiliary airfoil mounted ahead of the main airfoil in such a way as to assist in turning the airflow about the leading edge of the main airfoil. This accomplishment helps to increase the stall angle of attack of the main airfoil [4].

A leading-edge slat also uses a slot, or gap, between the main and auxiliary airfoils to allow airflow from the bottom of the device to mix with the airflow at the top of the main airfoil, thus re-energizing the airfoil's boundary layer. This boundary layer re-energization also helps to further delay the main airfoil's stall angle [4].

One should note that an aircraft's horizontal tail supplied a downward force (or "lift") to balance the aircraft in flight (Figure 6, page 16). Subsequently, a leading-edge slat must be placed in an inverted fashion (as opposed to a leading-edge slat on a wing) in order to continue and increase this downward force. Figure 8 shows the



WING LEADING-EDGE SLAT



HORIZONTAL TAIL LEADING-EDGE SLAT

Figure 8. Wing Leading-Edge and Horizontal Tail Leading-Edge Slats

difference between a wing's leading-edge slat and a slat for a horizontal tail.

In addition to improving stall characteristics, a leading-edge slat would also produce a larger effective surface area of the horizontal tail. From Equation (9), this area increase causes the aircraft's horizontal tail volume coefficient to increase. This volume coefficient increase in turn increases the horizontal tail's contribution to the static longitudinal stability of the aircraft, as can be seen from Equation (5).

Because use of a leading-edge slat on the horizontal tail of the Jetwing would improve both its stability and tail stall characteristics and would be quite simple to install, such a device will be more closely examined for its overall effect on the Jetwing. However, due to its more simple construction, a leading-edge slat for the horizontal tail of the Jetwing should remain in a fixed position.

Sisterman [12] has designed a leading-edge slat for use on the horizontal tail of the Ball-Bartoe Jetwing. The slat is basically simple, consisting primarily of sheet metal bent around steel tubing, and crimped to achieve a slat deflection of approximately 20 degrees. The slat extends through the stabilizer portion of the horizontal tail, but does not cover the shielded horn portion of the elevator. Figures 9 and 10 show the Sisterman slat for the maximum chord position, as well as a planform view of the slat, respectively [12].

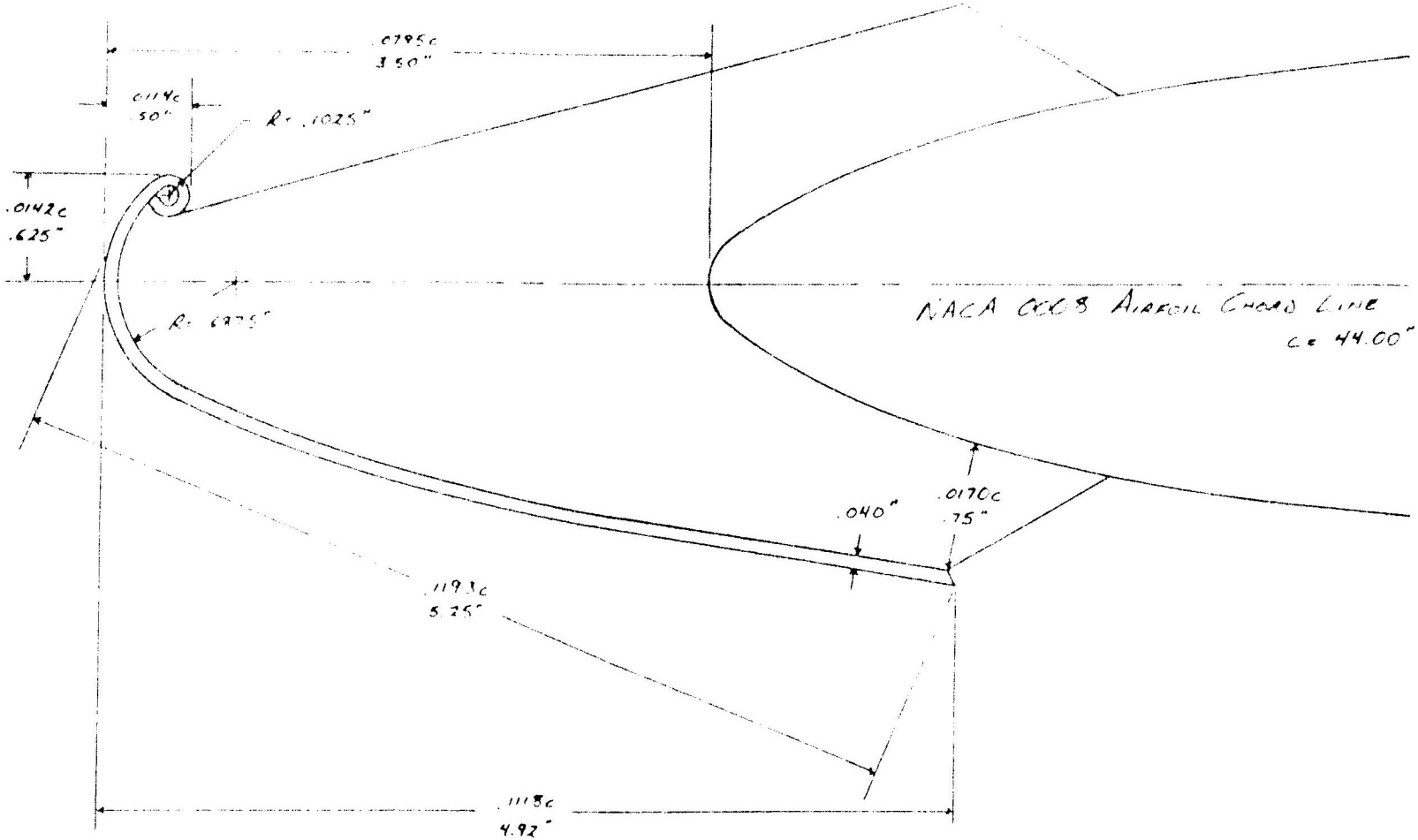


Figure 9. Sisterman's Proposed Thin Slat Design at the Maximum Chord Position [12]

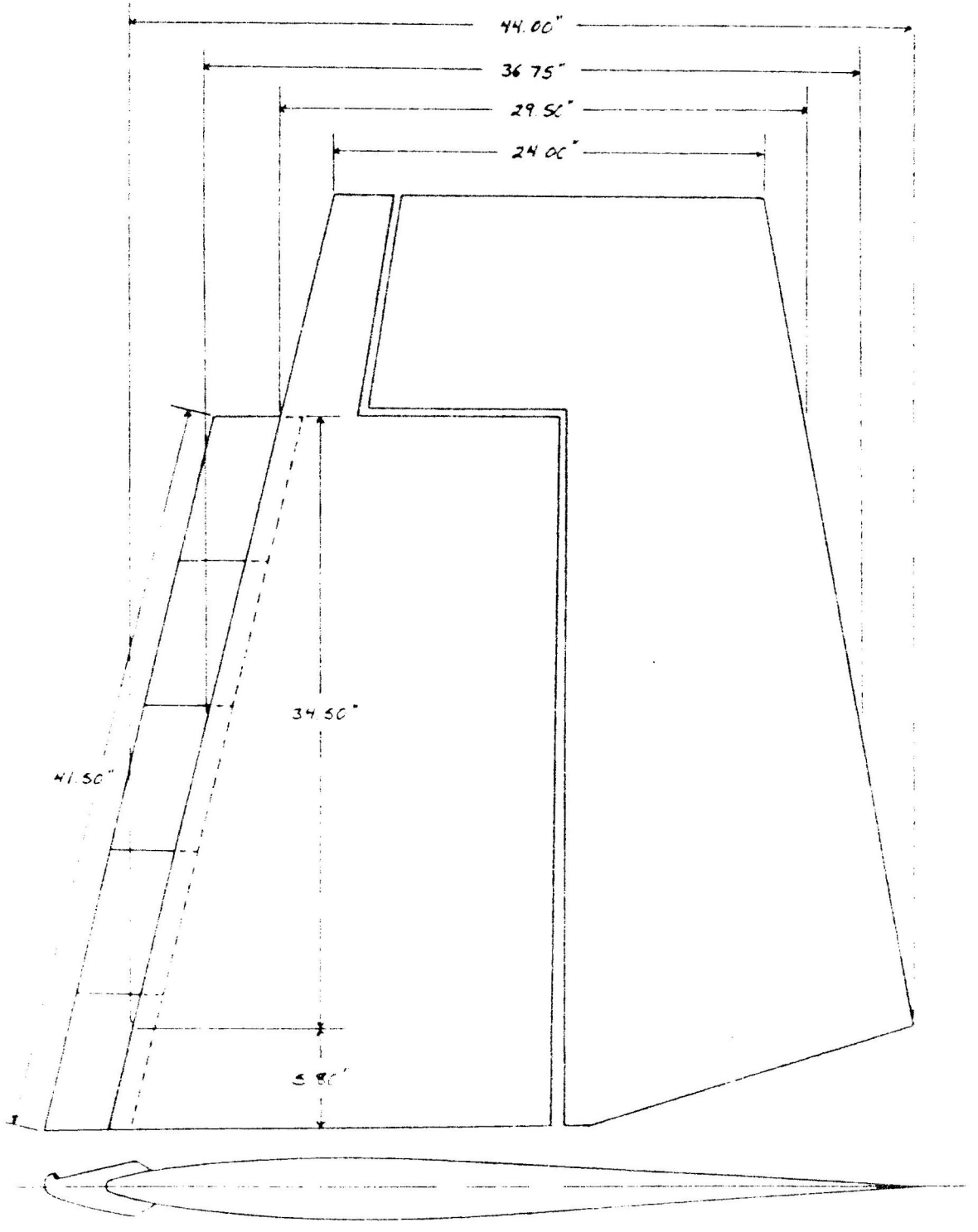


Figure 10. Planform View of the Horizontal Tail with the Proposed Modification of the Sisterman Slat [12]

Addition of Leading-Edge Droop

Another possible design solution to the Jetwing's problems of horizontal tail stall and static longitudinal instability is the use of leading-edge droop on the aircraft's horizontal tail. Leading-edge droop is basically a chord and camber extension device; the leading edge of the lifting surface is enlarged and deflected (upward for a horizontal tail lifting surface) to help turn the airflow about the lifting surface. In this respect, leading-edge droop is similar to a leading-edge slat configuration. However, unlike the leading-edge slat, leading-edge droop provides no slot for re-energizing the boundary layer of the lifting surface.

Addition of leading-edge droop will alleviate the problems of the Jetwing in much the same way as a leading-edge slat. Through the addition of camber and chord extension (and thus effective surface area increase), the Jetwing's tail stall and stability problems should be diminished. However, because of its lack of a boundary layer re-energization device such as a slot, the leading-edge droop configuration would probably alleviate these problems to a lesser extent than would a leading-edge slat. This difference is primarily due to the fact that the droop configuration generally produces a smaller stall angle of attack than does the leading-edge slat [13].

However, a leading-edge droop configuration, because of its smaller size, would probably produce less drag than a leading-edge slat. In addition, because the droop arrangement is basically a chord

extension, it would be much simpler to design and fabricate than a slat arrangement. Therefore, a leading-edge droop arrangement will be tested as a possible solution to the Jetwing's tail stall and stability problems. The leading edge droop modification is basically an airfoil extension of 2 inches throughout the same span as the Sisterman slat. A depiction of this arrangement can be found in Figure 11.

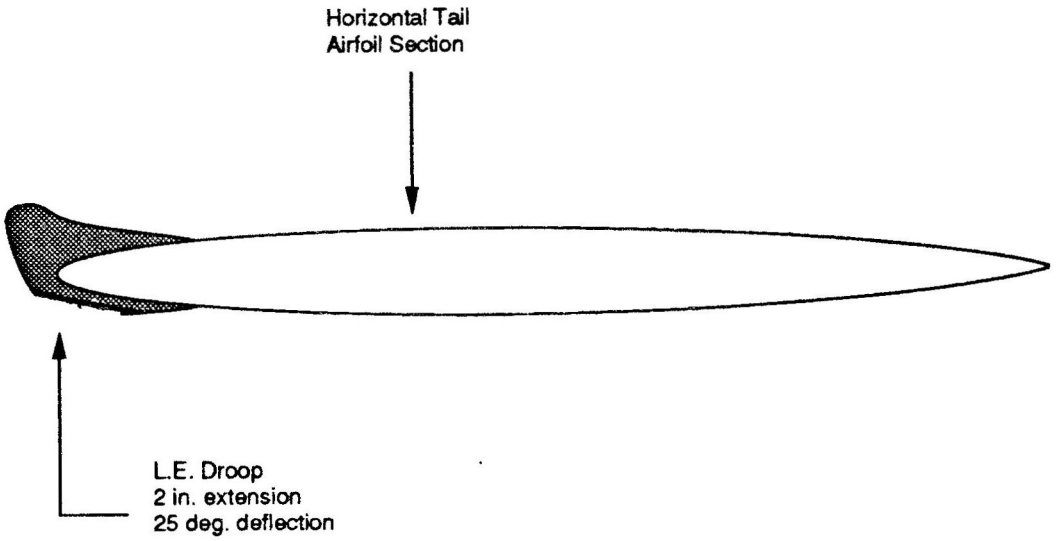


Figure 11. Proposed Leading-Edge Droop Modification for Jetwing Horizontal Tail

CHAPTER V

WIND-TUNNEL TESTS OF PROPOSED MODIFICATIONS

Introduction

The University of Tennessee Space Institute (UTSI) currently operates a low-speed wind tunnel with a test section measuring 14 inches high, 20 inches wide, and 36 inches long. The wind tunnel is used to test aerodynamic models at speeds up to 100 miles per hour. Because of its low-speed capabilities and dimensions, the UTSI low-speed wind tunnel is well suited for testing possible modifications to the Jetwing's horizontal tail [14].

Description of the Test Model

Because of the size limitations of the UTSI low-speed wind tunnel test section, it was necessary to build the test model to quarter-scale of the actual Ball-Bartoe Jetwing horizontal tail. In addition, the model represents only a half-span portion of the Jetwing's horizontal tail.

The wind-tunnel model of the Jetwing's horizontal tail is made of molded polystyrene foam with an epoxy and milled glass skin. The elevator portion of the model is connected to the horizontal stabilizer by a simple hinge mechanism. The hinge may be locked in place in order to hold elevator deflections constant. In addition, attachments points are located near the leading edge of the horizontal stabilizer so that outboard, inboard, and full span slat and droop modifications may be

easily applied. A picture of the test model used is shown in Figure 12.

Test Procedure

A total of three model configurations were tested for this investigation: the plain model (with no modifications), full span leading-edge slat device on the stabilizer (as designed by Sisterman) [14], and a full-span droop arrangement. A test matrix, showing all configurations tested, is shown in Table 5.

The wind tunnel model was used during flow visualization tests, so that flow characteristics about the model could be analyzed. Photographs of the model were taken at each stabilized angle of attack during each test run. Elevator deflections of 0, 10, 20, and 30 degrees were tested for each of the three model configurations.

In addition, lift and drag data were recorded for the untufted model by mounting the model on a 4-strain gage balance. Each angle of attack (during all tests) was approached from above and below to examine for possible hysteresis effects. Lift and drag data were reduced by the method described by Tietz [15].

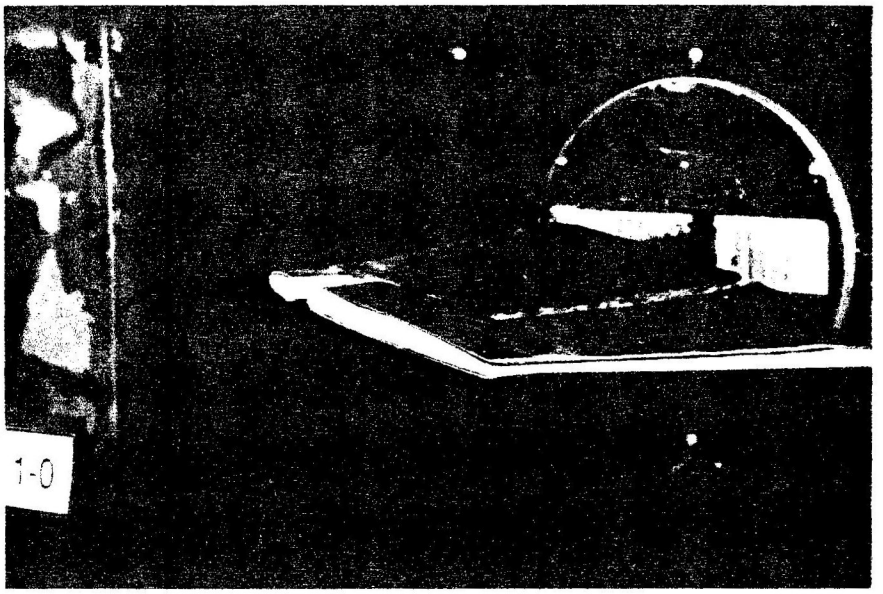


Figure 12. Quarter-Scale Model of Jetwing Half-Tail

Table 5. Test Matrix of Jetwing Tail Model

Number	Configuration
1.0	Plain; no leading edge devices
2.0	Full-span Sisterman slat
3.0	Full-span leading-edge droop

CHAPTER VI

RESULTS AND DISCUSSION

Photographs during each test run can be found in Figures 13 through 24. Lift coefficient versus angle-of-attack plots (for various elevator deflections) for each modification are shown in Figures 25 through 27. A characteristic drag polar for each modification (for zero degree elevator deflection) can be found in Figure 28.

Horizontal Tail Stall

Kimberlin [8] has derived a method that predicts the horizontal tail lift coefficient required for stabilized flight. The horizontal tail lift coefficient, C_{L_t}, is defined as:

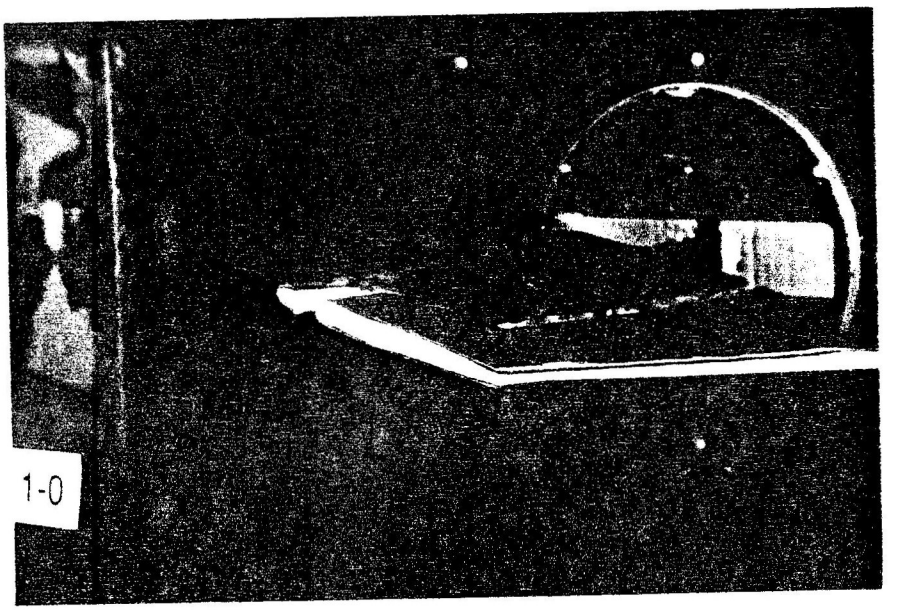
$$C_{L_t} = \frac{\alpha_{(s)}\left(\frac{\partial C_L}{\partial \alpha}\right)_{(s)}\left(h - \xi_{\alpha(s)}\right) + \delta_{(s)}\left(\frac{\partial C_L}{\partial \delta}\right)_{(s)}\left(h - \xi_{(s)}\right)}{V_H} \tag{10}$$

where: $\alpha_{(s)}$ = stabilized angle of attack

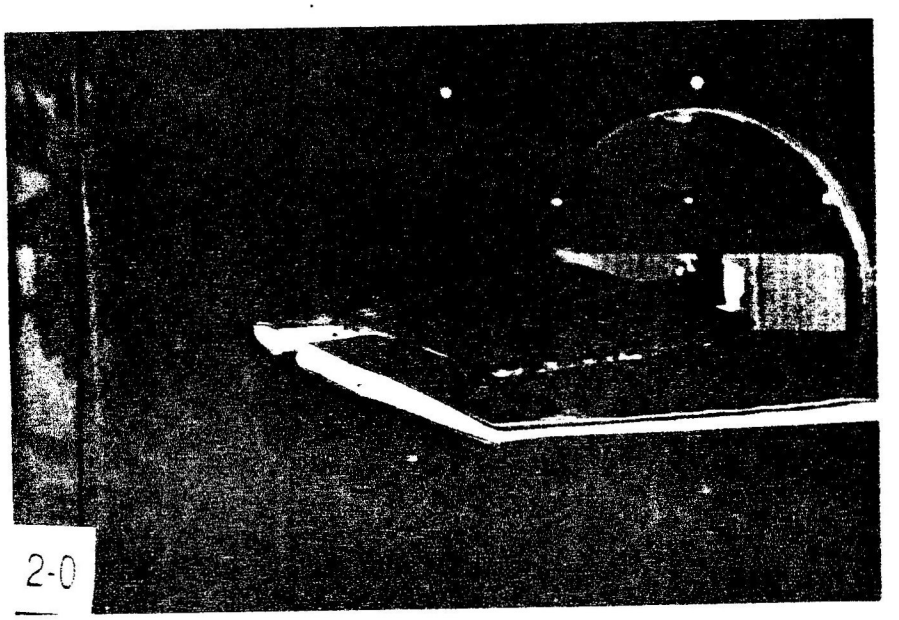
$(\partial C_L/\partial \alpha)_{(s)}$ = stabilized partial derivative of lift coefficient with respect to angle of attack

h = location of center of gravity (% M.A.C.)

$\xi_{\alpha(s)}$ = stabilized aerodynamic center due to angle of attack

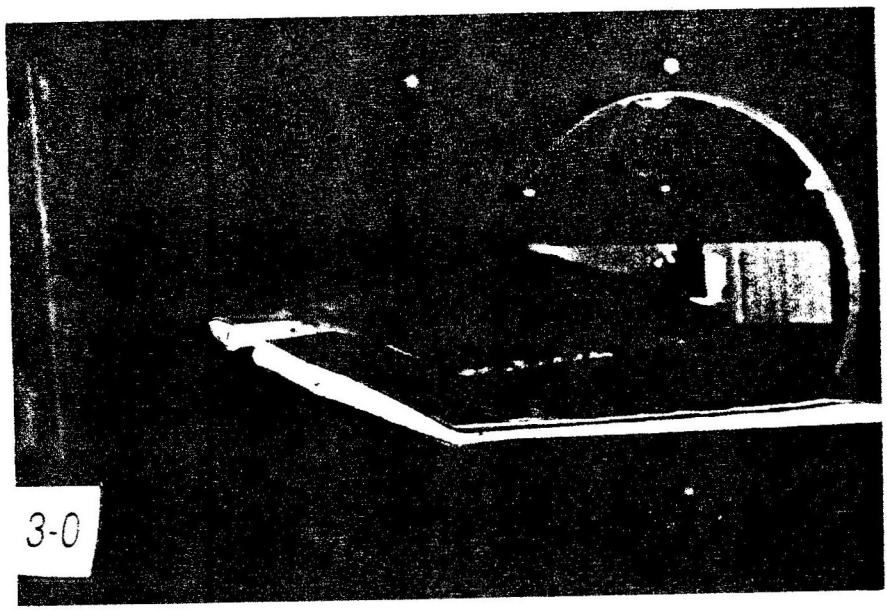


a. $\alpha_T = 10°$



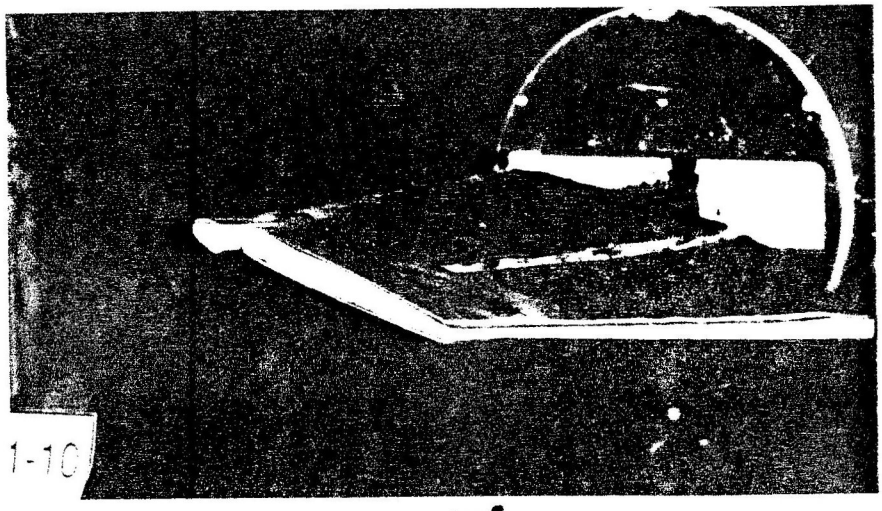
b. $\alpha_T = 13°$

Figure 13. Flow Visualization of Jetwing Horizontal Tail Model with No Modifications and 0-Degree Elevator Deflection

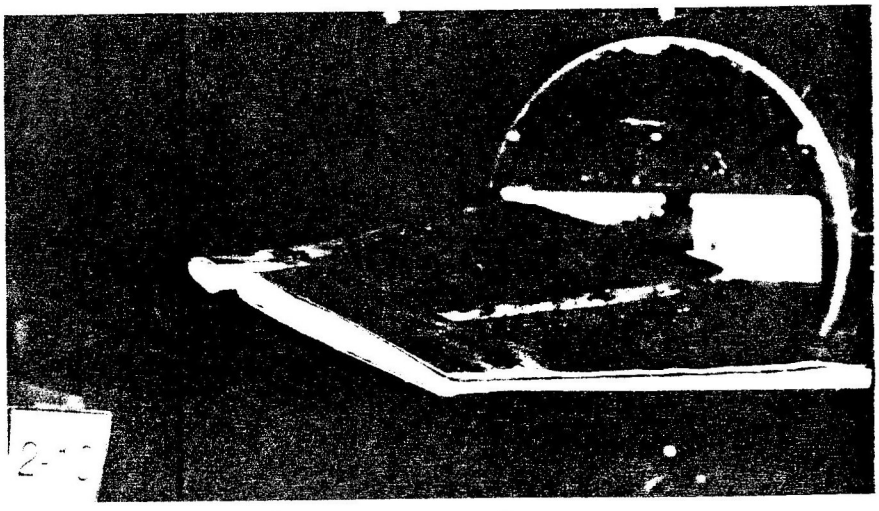


c. $\alpha_T = 15^\circ$

Figure 13. Concluded

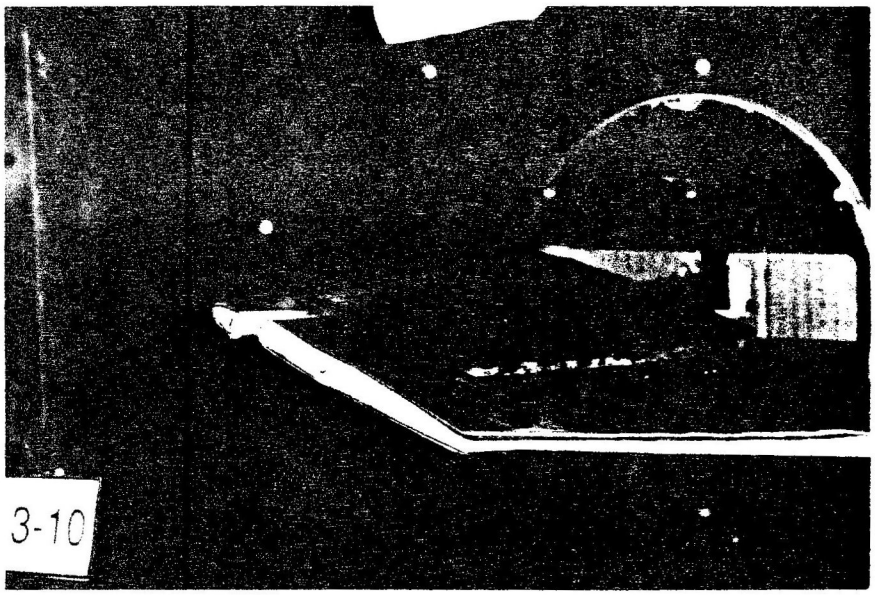


a. $\alpha_T = 10°$



b. $\alpha_T = 13°$

Figure 14. Flow Visualization of Jetwing Horizontal Tail Model with No Modifications and 10-Degree Elevator Deflection

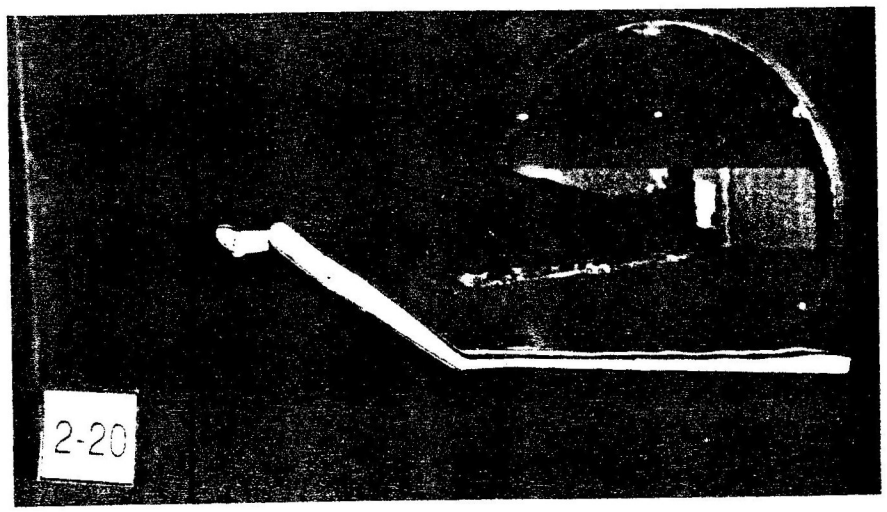


c. $\alpha_T = 15^\circ$

Figure 14. Concluded

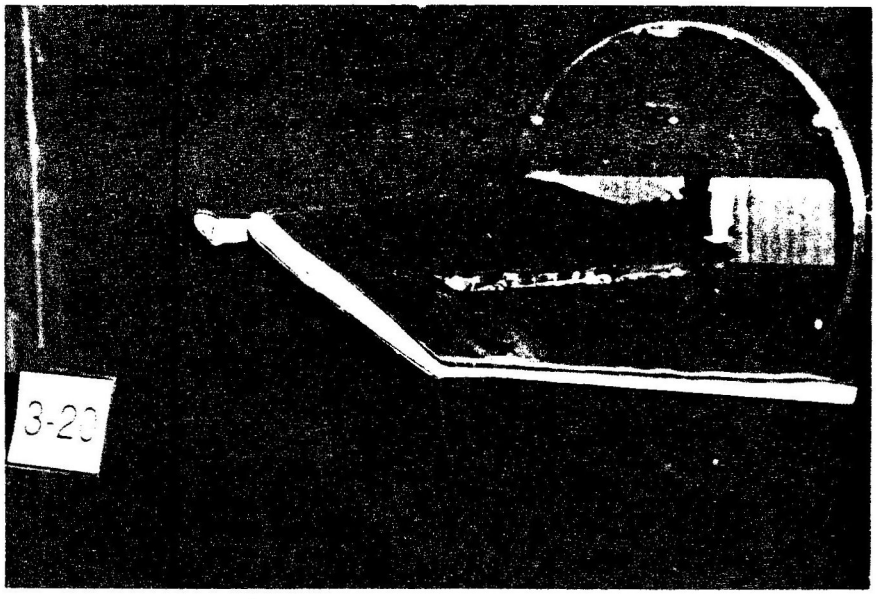


a. $\alpha_T = 10°$



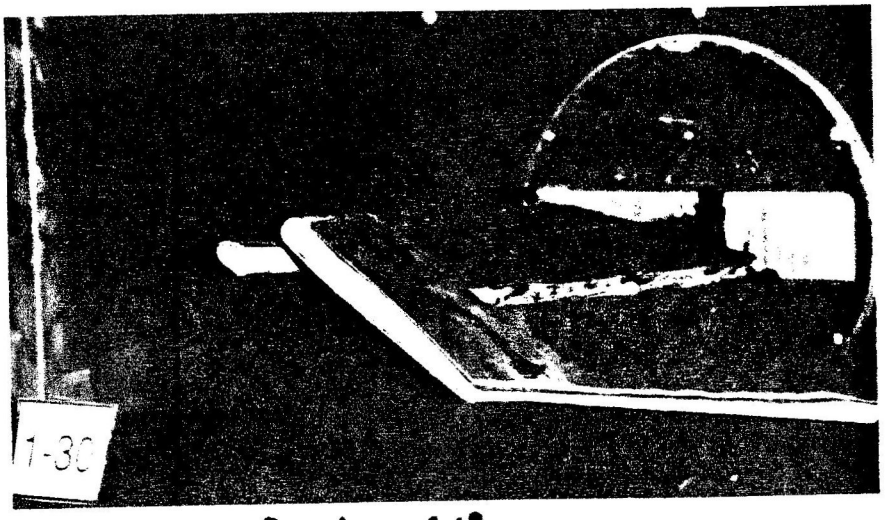
b. $\alpha_T = 13°$

Figure 15. Flow Visualization of Jetwing Horizontal Tail Model with No Modifications and 20-Degree Elevator Deflection

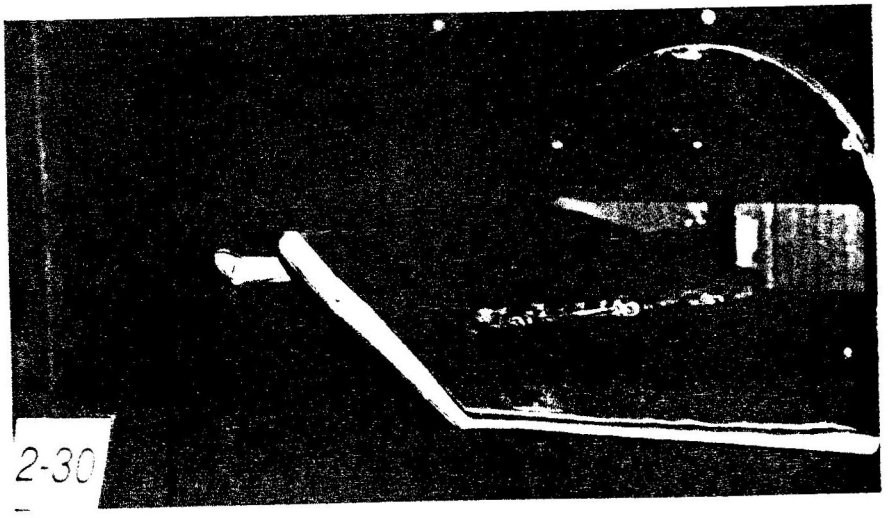


c. $\alpha_T = 15°$

Figure 15. Concluded

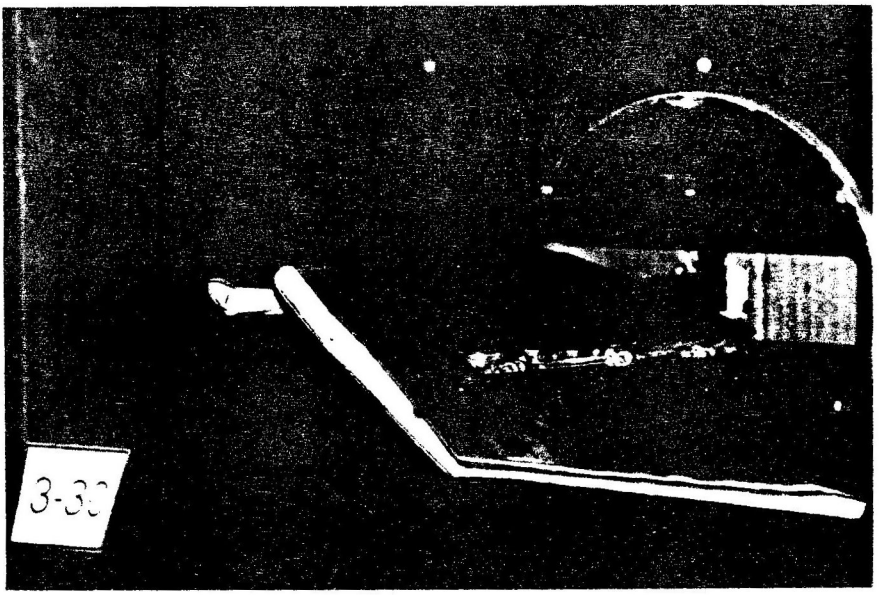


a. $\alpha_T = 10°$



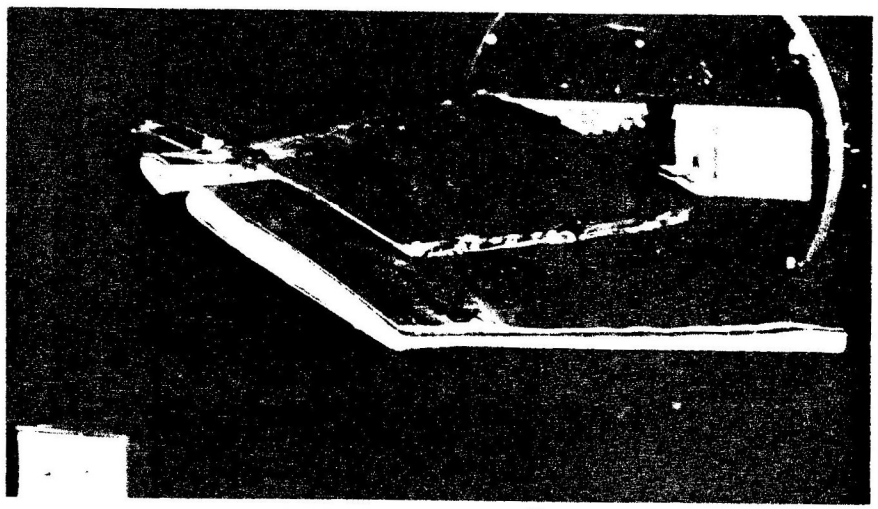
b. $\alpha_T = 13°$

Figure 16. Flow Visualization of Jetwing Horizontal Tail Model and 30-Degree Elevator Deflection

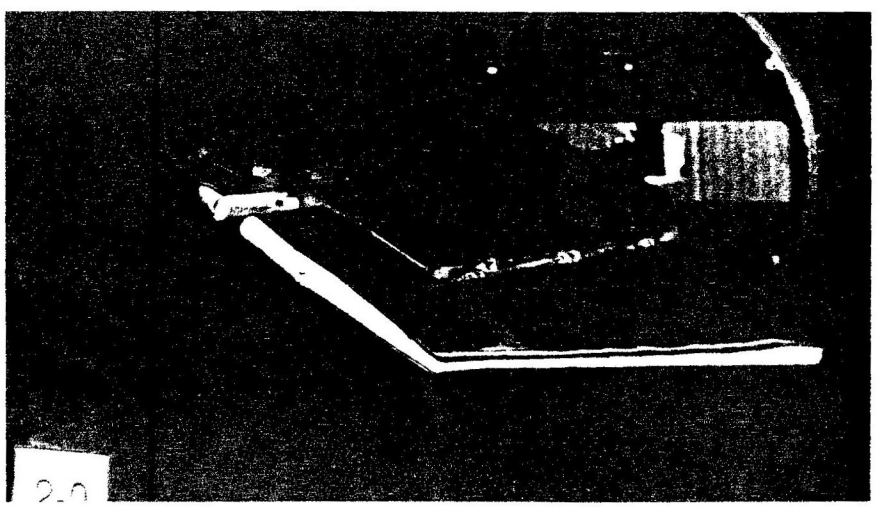


c. $\alpha_T = 15°$

Figure 16. Concluded

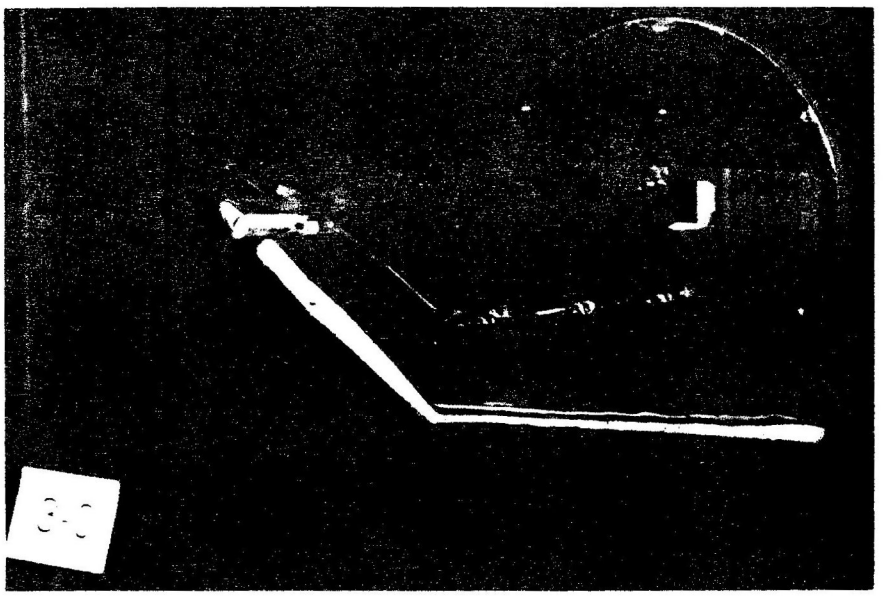


a. $\alpha_T = 20°$



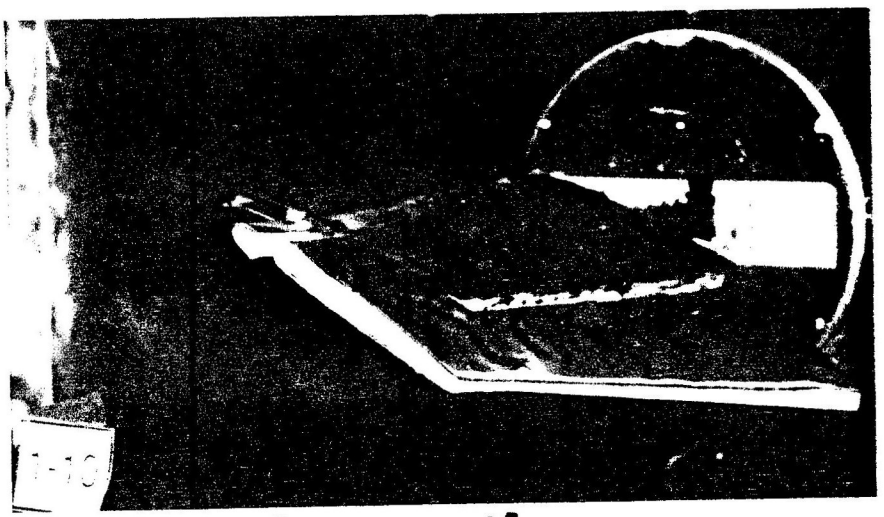
b. $\alpha_T = 25°$

Figure 17. Flow Visualization of Jetwing Horizontal Tail Model with Leading-Edge Slat and 0-Degree Elevator Deflection

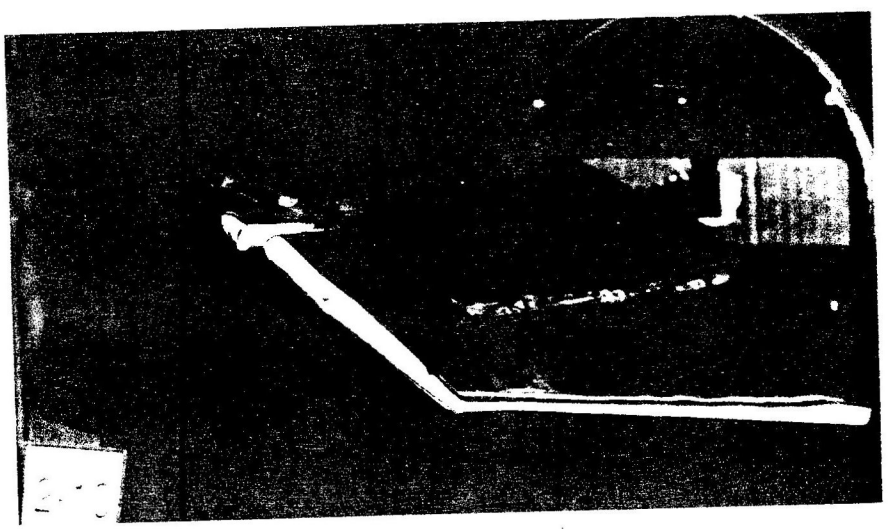


c. $\alpha_T = 30^\circ$

Figure 17. Concluded

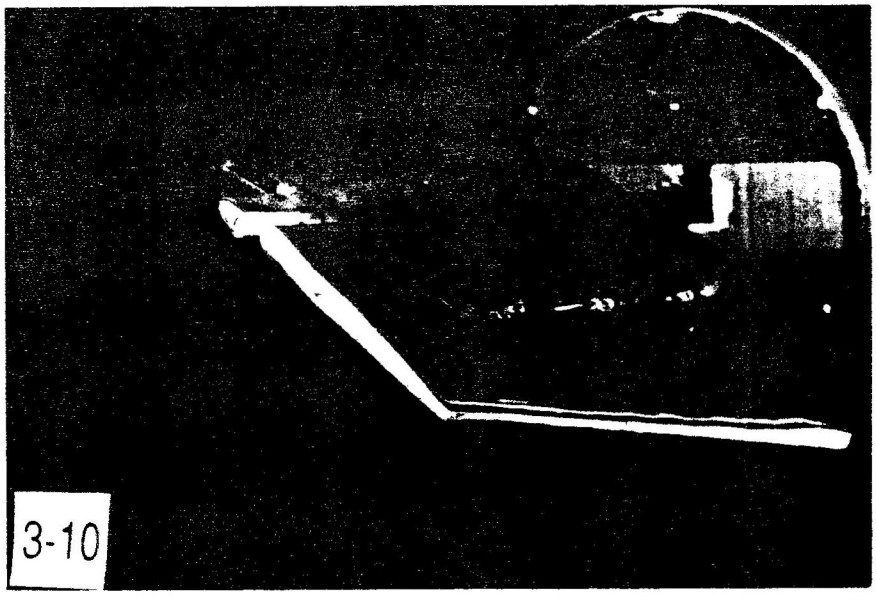


a. $\alpha_T = 20°$



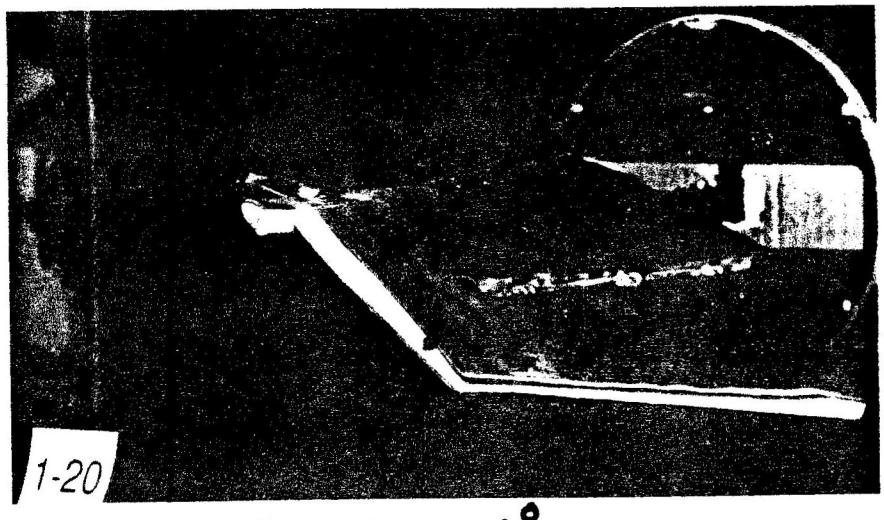
b. $\alpha_T = 20°$

Figure 18. Flow Visualization of Jetwing Horizontal Tail Model with Leading-Edge Slat and 10-Degree Elevator Deflection

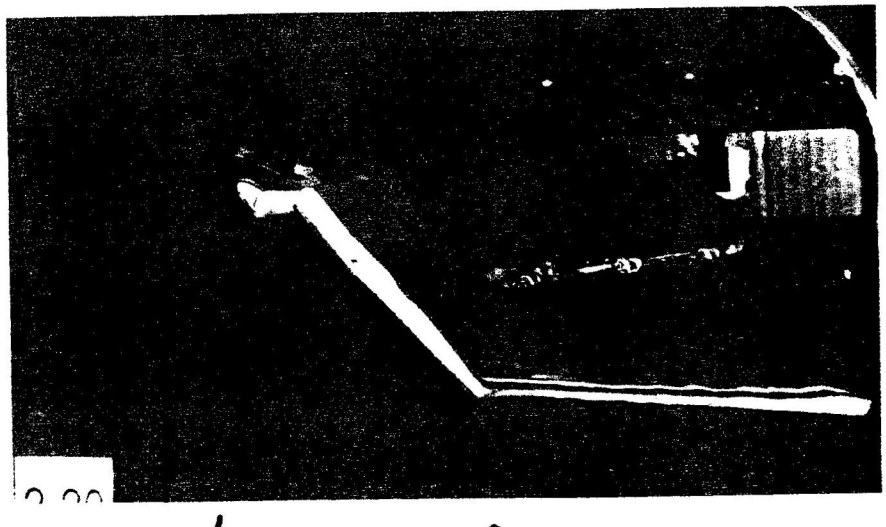


c. $\alpha_T = 30^\circ$

Figure 18. Concluded

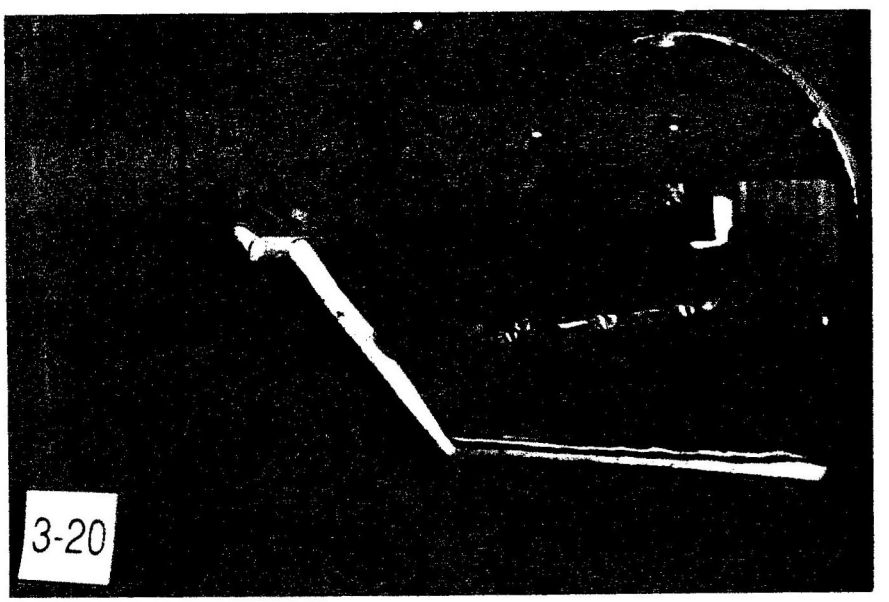


a. $\alpha_T = 20°$



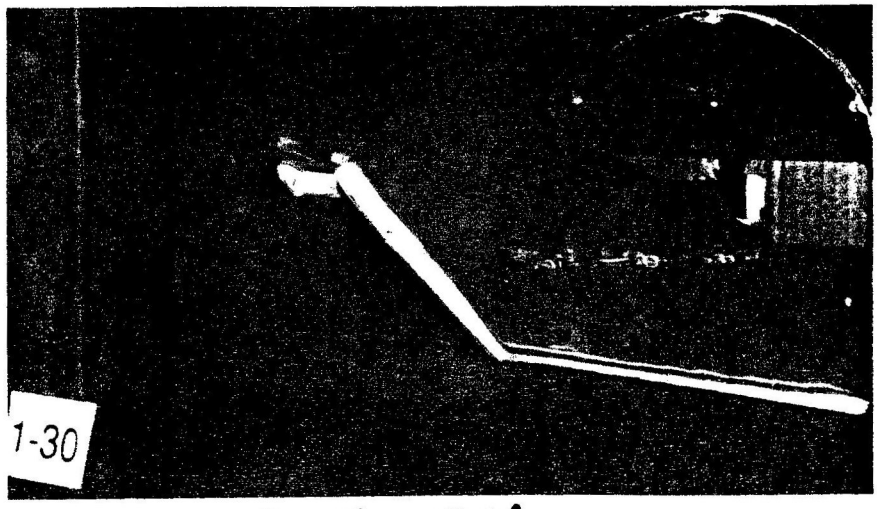
b. $\alpha_T = 25°$

Figure 19. Flow Visualization of Jetwing Horizontal Tail Model with Leading-Edge Slat and 20-Degree Elevator Deflection

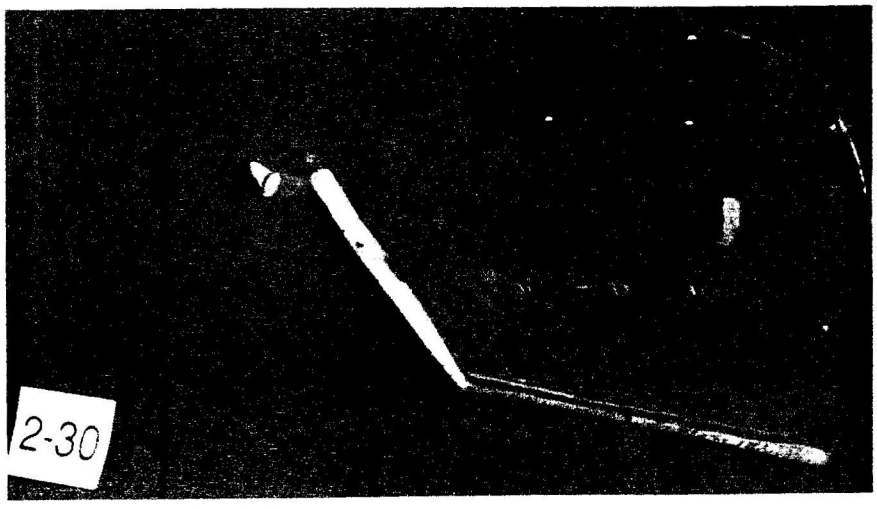


c. $\alpha_T = 30^\circ$

Figure 19. Concluded

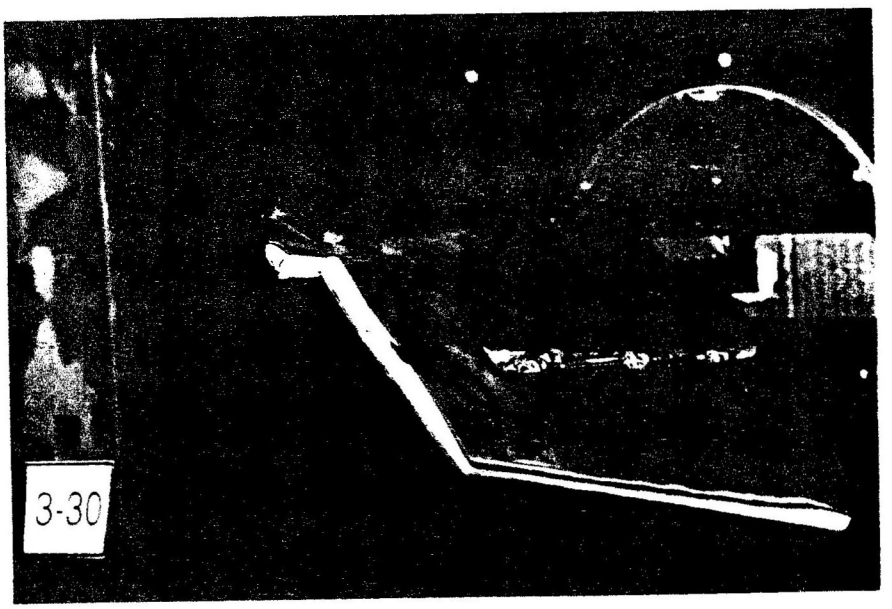


a. $\alpha_T = 20°$



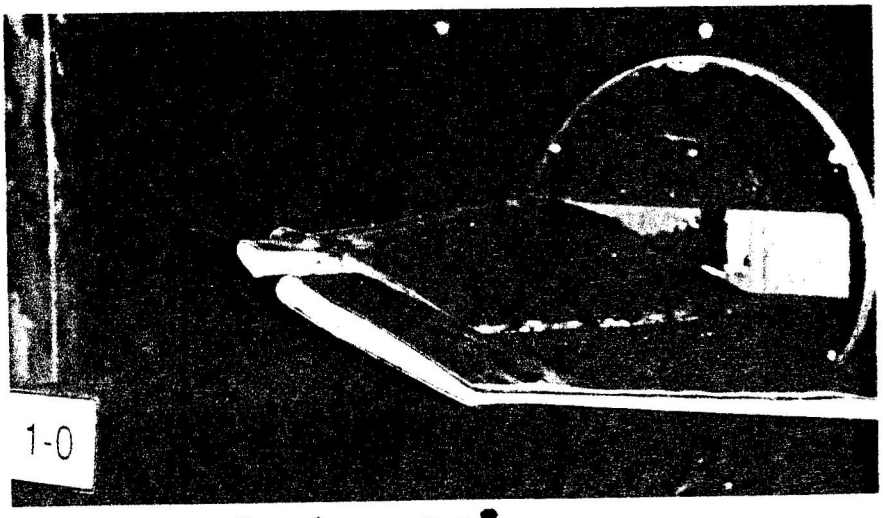
b. $\alpha_T = 25°$

Figure 20. Flow Visualization of Jetwing Horizontal Tail Model with Leading-Edge Slat and 30-Degree Elevator Deflection

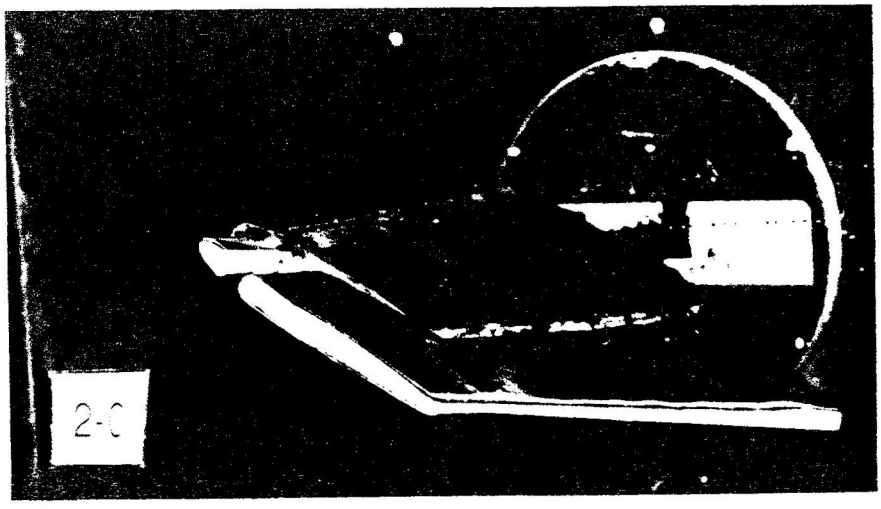


c. $\alpha_T = 30^\circ$

Figure 20. Concluded

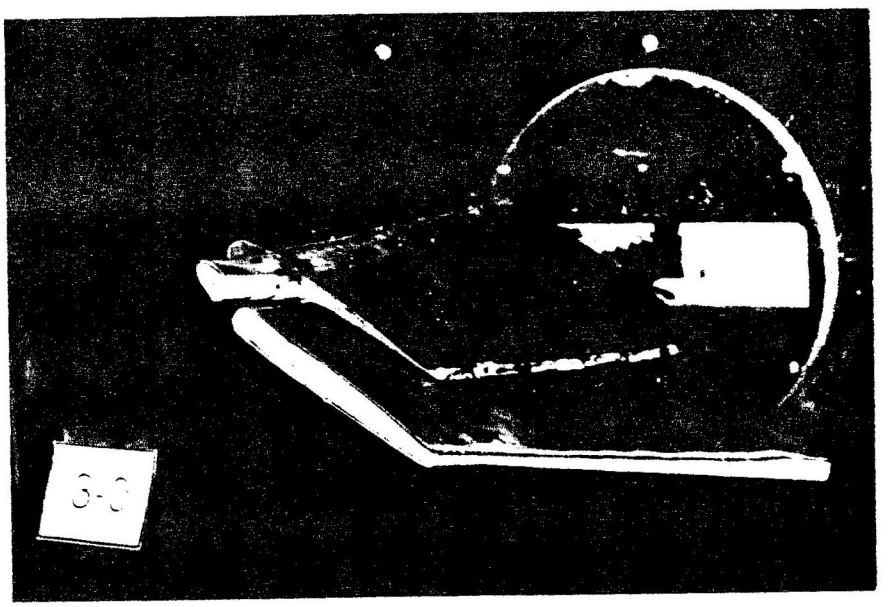


a. $\alpha_T = 20°$



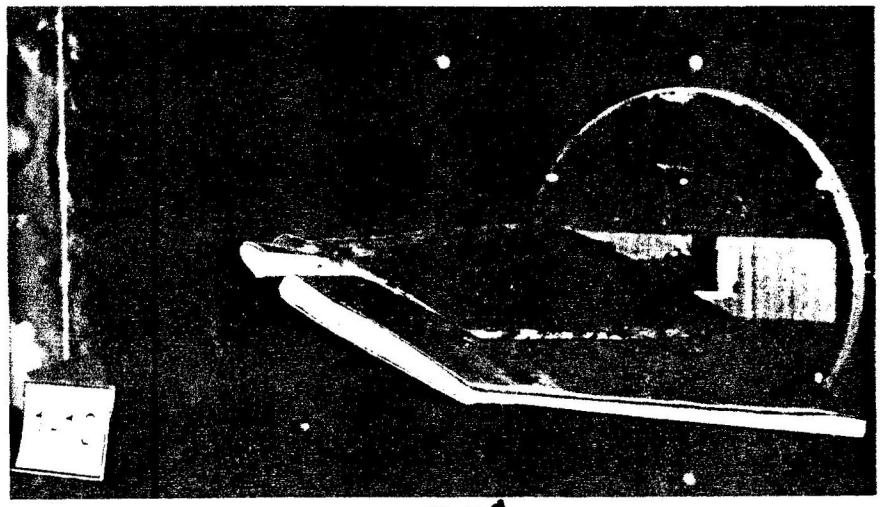
b. $\alpha_T = 25°$

Figure 21. Flow Visualization of Jetwing Horizontal Tail Model with Leading-Edge Droop and 0-Degree Elevator Deflection

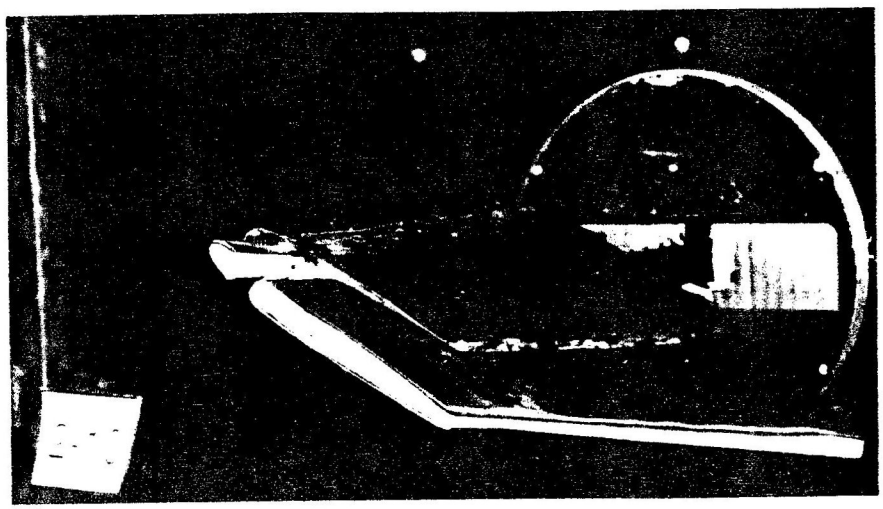


c. $\alpha_T = 30°$

Figure 21. Concluded

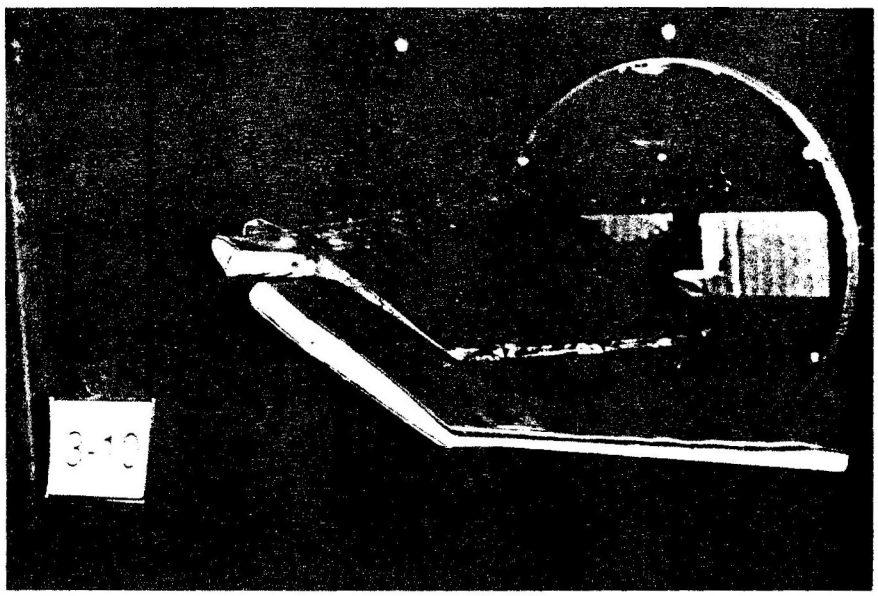


a. $\alpha_T = 20^\circ$



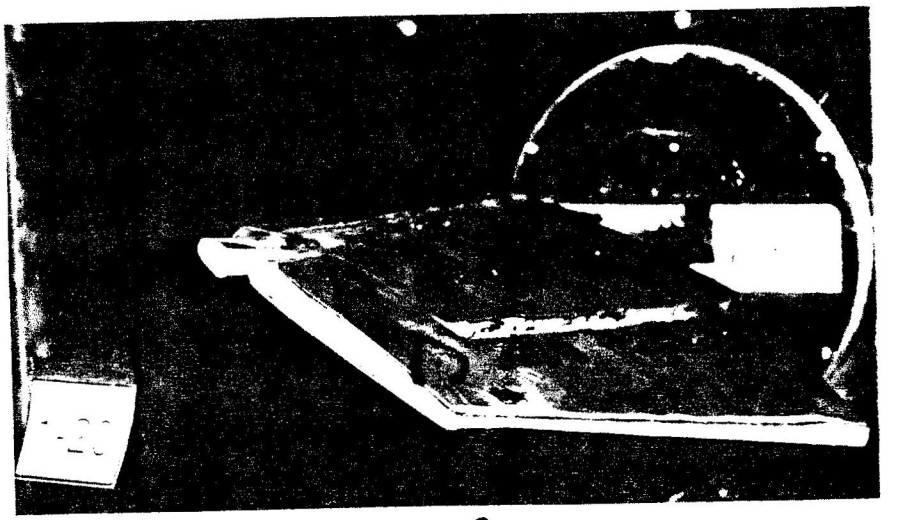
b. $\alpha_T = 25^\circ$

Figure 22. Flow Visualization of Jetwing Horizontal Tail Model with Leading-Edge Droop and 10-Degree Elevator Deflection

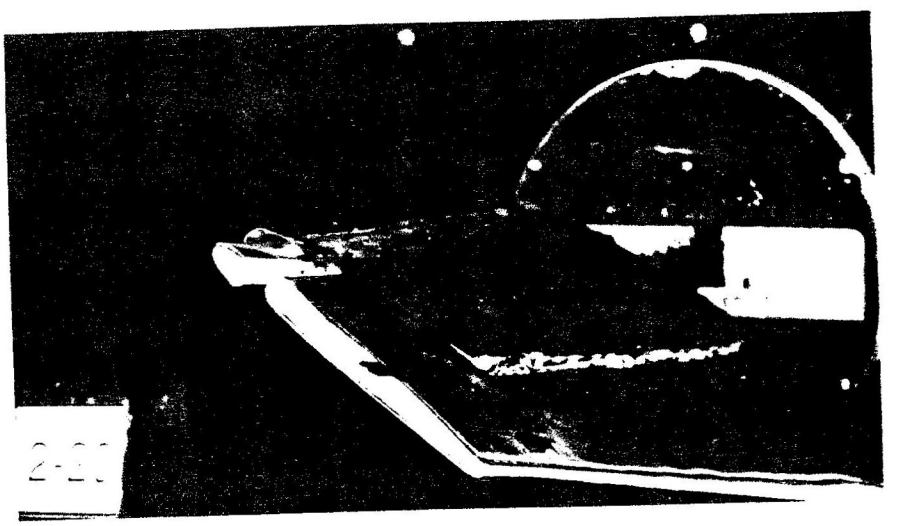


c. $\alpha_T = 30°$

Figure 22. Concluded

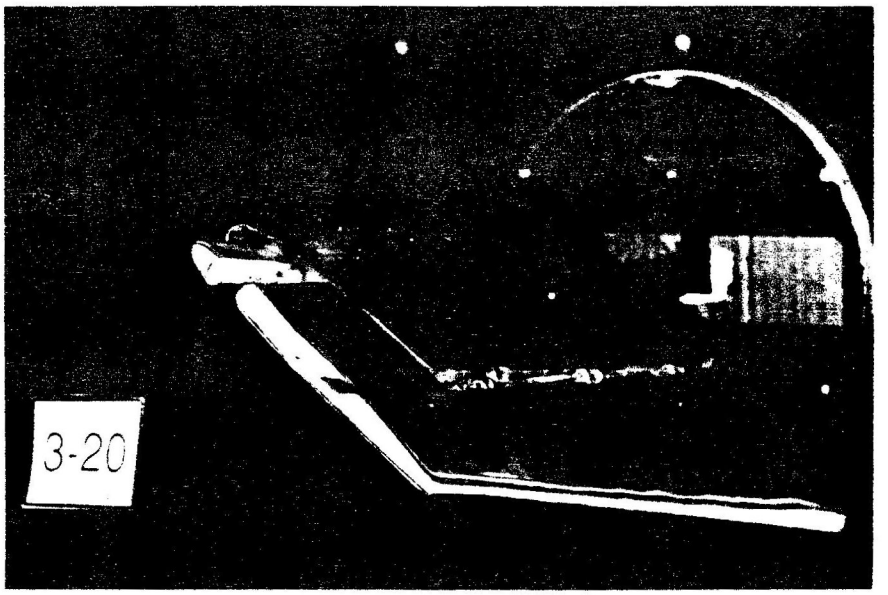


a. $\alpha_T = 20°$



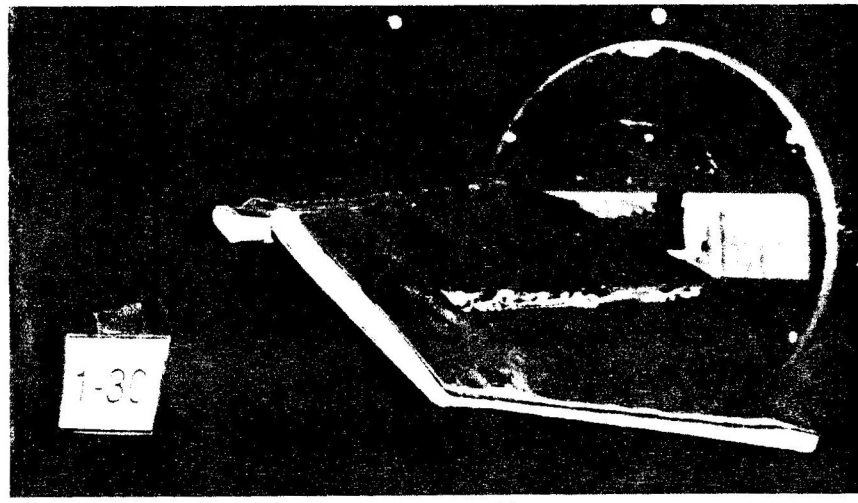
b. $\alpha_T = 25°$

Figure 23. Flow Visualization of Jetwing Horizontal Tail Model with Leading-Edge Droop and 20-Degree Elevator Deflection

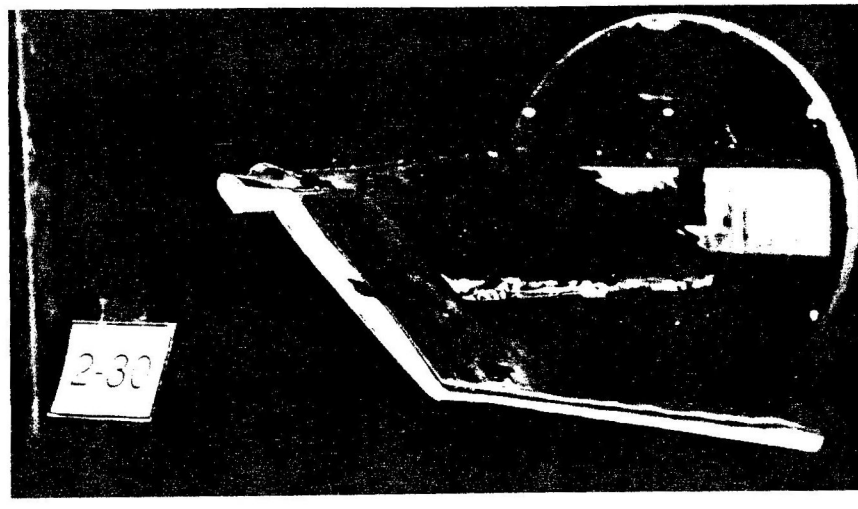


c. $\alpha_T = 30^\circ$

Figure 23. Concluded

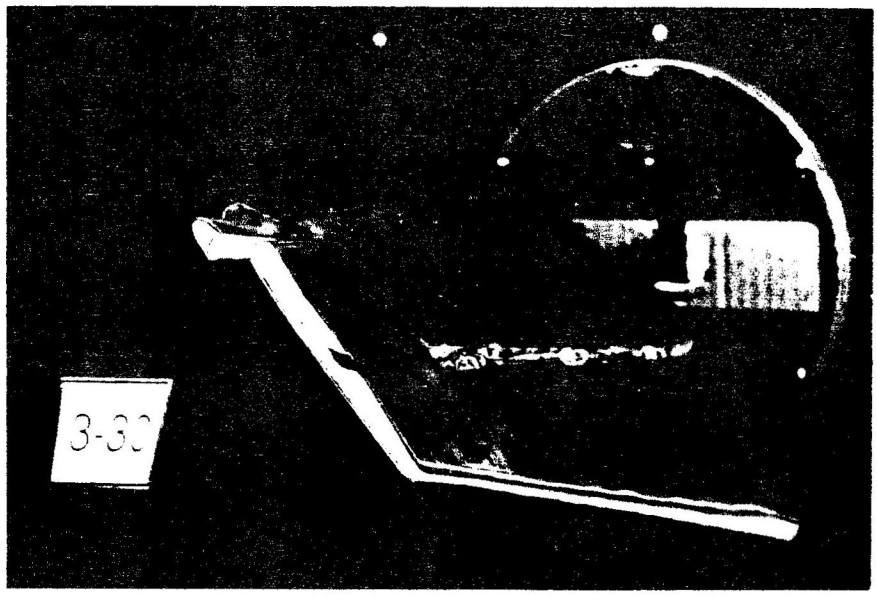


a. $\alpha_T = 20°$



b. $\alpha_T = 25°$

Figure 24. Flow Visualization of Jetwing Horizontal Tail Model with Leading-Edge Droop and 30-Degree Elevator Deflection



c. $\alpha_4 = 30°$

Figure 24. Concluded

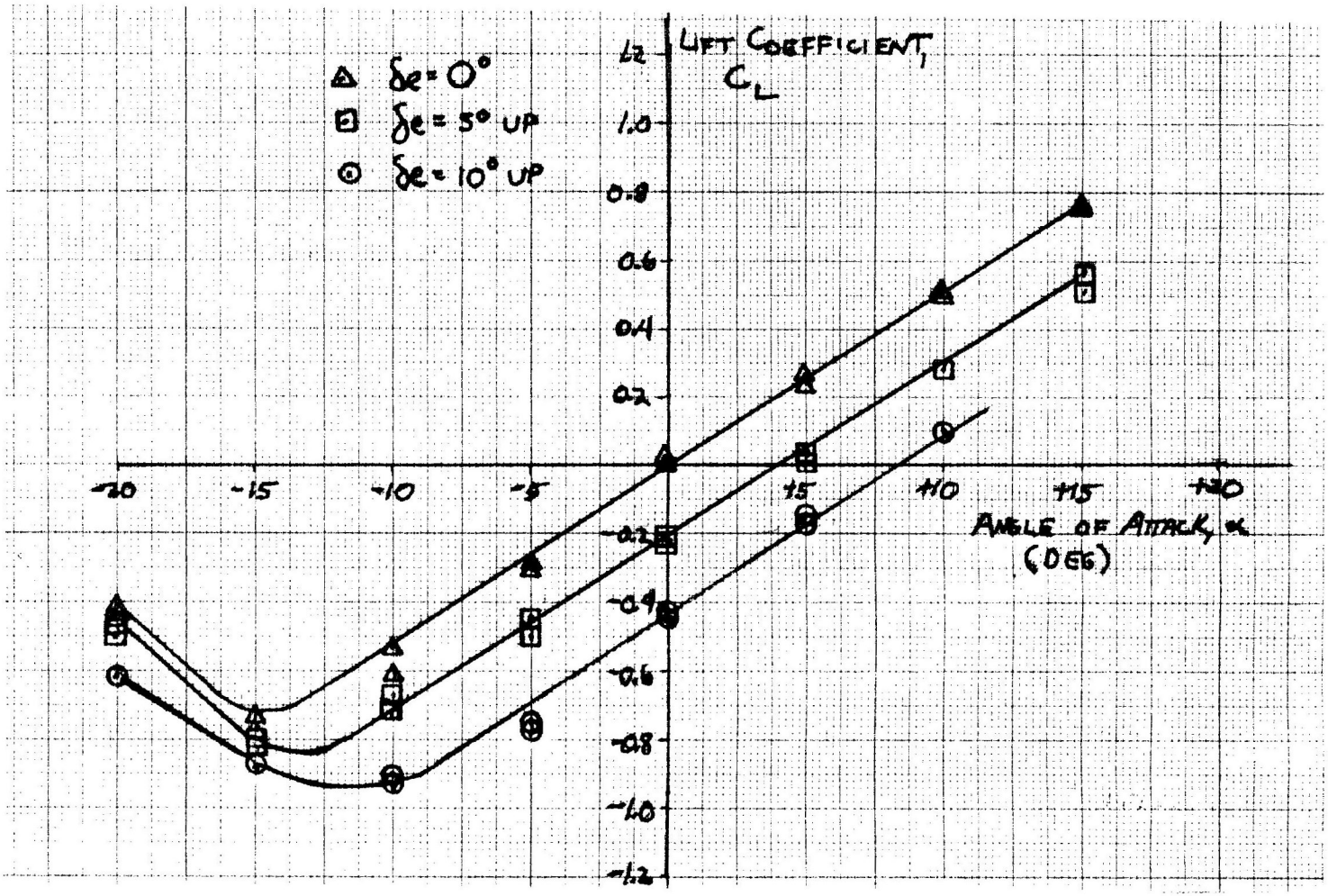


Figure 25. Lift Coefficient versus Angle of Attack for Plain Model

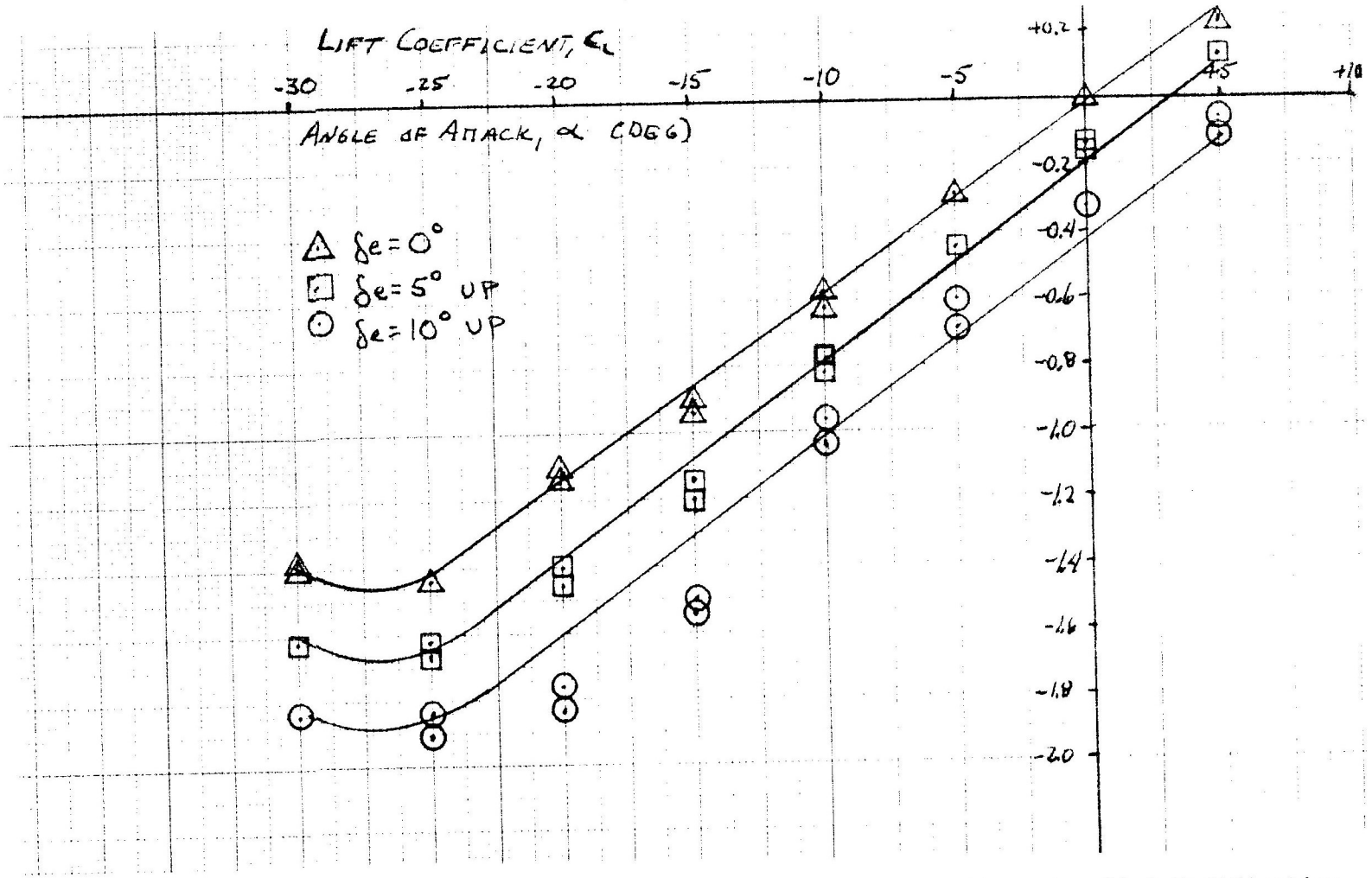


Figure 26. Lift Coefficient versus Angle of Attack for Leading-Edge Slat Modification

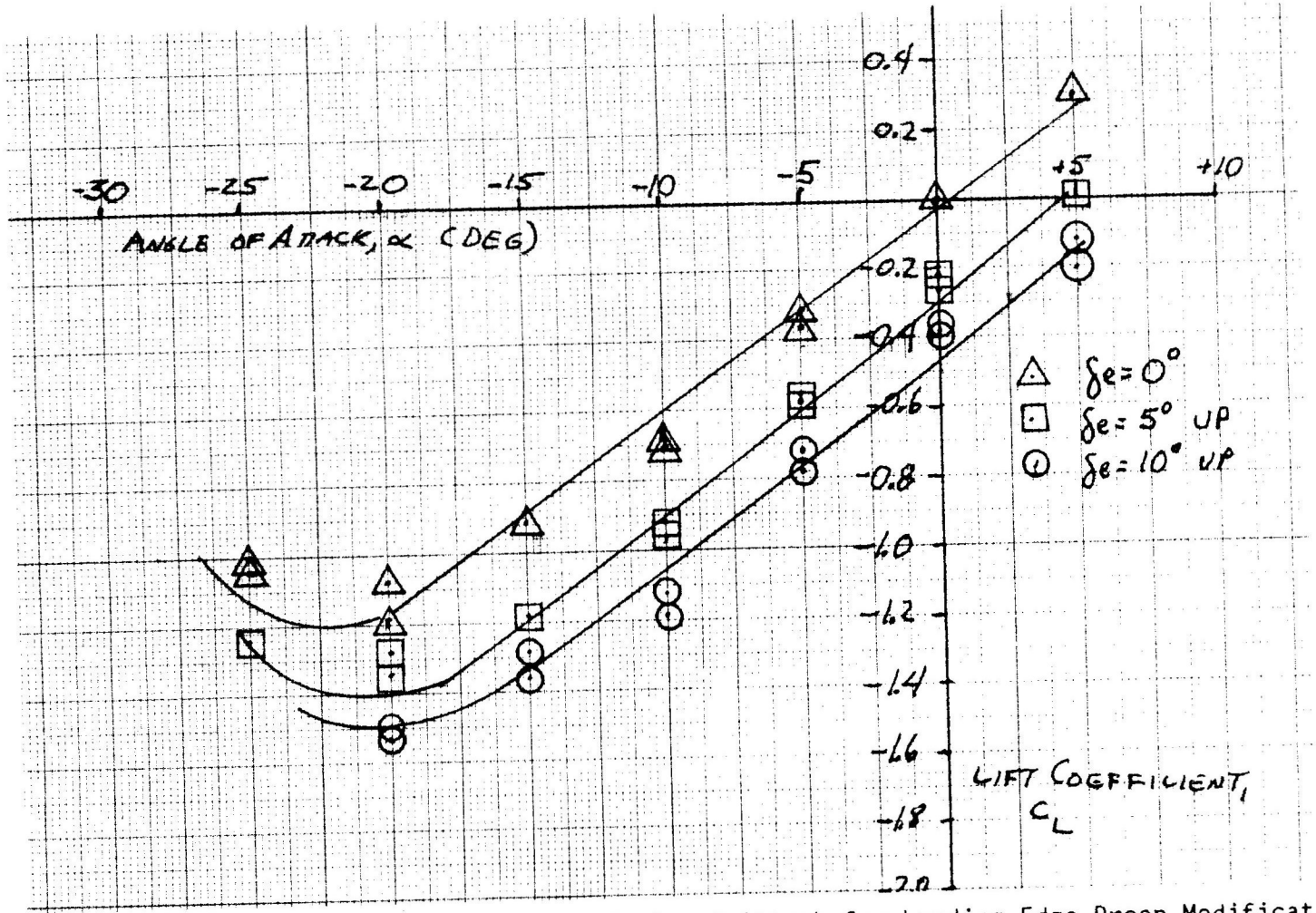


Figure 27. Lift Coefficient versus Angle of Attack for Leading-Edge Droop Modification

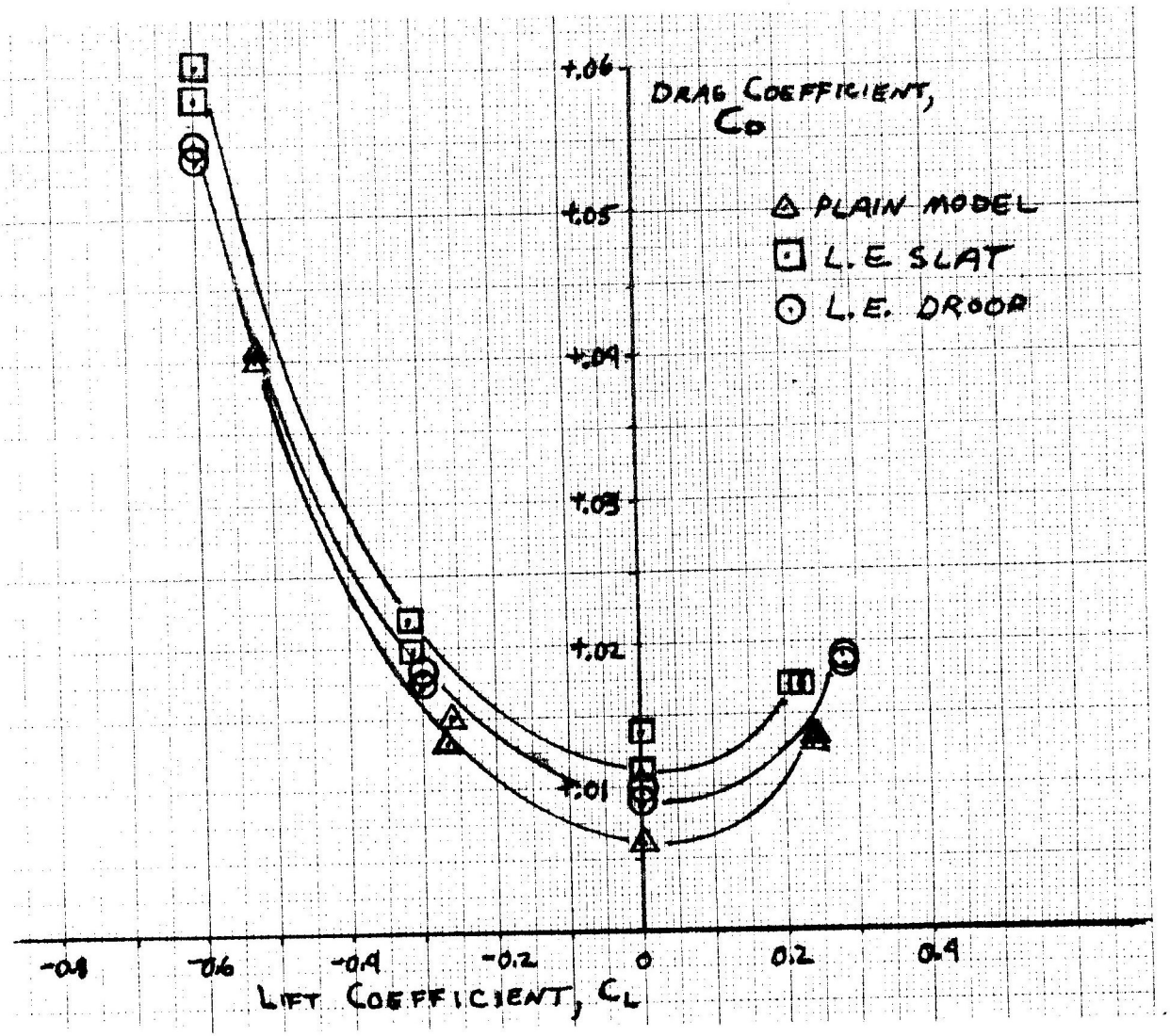


Figure 28. Characteristic Drag Polar for All Test Models

$\xi_{\delta(s)}$ = stabilized aerodynamic center due to Upper Surface Blowing effects

$(\partial C_L/\partial\delta)_{(s)}$ = stabilized partial derivative of lift coefficient with respect to blowing deflection

V_H = horizontal tail volume coefficient

The partial derivative with respect to angle of attack term is [8]:

$$\left(\frac{\partial C_L}{\partial \alpha}\right)_{(s)} = a_w \left| 1 + 0.151 \left(C'_{J(s)}\right)^{1/2} + 0.219 \left(C'_{J(s)}\right) \right| \tag{11}$$

where: a_w = wing lift-curve slope (for no blowing)

$C'_{J(s)}$ = stabilized corrected blowing coefficient

The partial derivative with respect to blowing deflection term in Equation (10) is given by the equation [8]:

$$\left(\frac{\partial C_L}{\partial \delta}\right)_{(s)} = \left| 4\pi \left(C'_{J(s)}\right) \left(1 + 0.151 \left(C'_{J(s)}\right)^{1/2} + 0.139\, C'_{J(s)} \right) \right|^{1/2} \tag{12}$$

Both Equations (11) and (12) make use of the corrected blowing coefficient, $C'_{J(s)}$. This correction arises because the entire wing area is not subject to blowing effects. This correction is defined as [8]:

$$C'_{J(s)} = C_{J(s)} \left(\frac{S}{S'} \right) \tag{13}$$

where: $C_{J(s)}$ = uncorrected blowing coefficient

S = wing area

S' = wing area subjected to blowing effects

The Ball-Bartoe Jetwing's wing area subject to blowing is one-half of its total wing area [1]. Therefore, the corrected blowing coefficient may be defined as:

$$C'_{J(s)} = 2\,C_{J(s)} \tag{14}$$

The aerodynamic center terms used in Equation (10) are defined by the equations [8]:

$$\xi_{\alpha(s)} = 0.25 - 0.01\,C'_{J(s)} \tag{15}$$

and

$$\xi_{\delta(s)} = 0.5 + 0.077\,(C'_{J(s)})^{1/2} \tag{16}$$

where $\xi_{\alpha}(s)$ and $\xi_{\delta}(s)$ are the aerodynamic centers in stabilized flight due to angle of attack and blowing deflection, respectively.

Using Solies' [2] data from Table 3, the largest lift coefficient the horizontal tail that the Jetwing is required to have for stabilized flight is -1.75.

Using Equations (10) through (16) for the leading-edge slat and droop configurations mentioned in Chapter V, and accounting for the changed tail area and tail arm that these modifications yield, the maximum horizontal tail lift coefficient required of the Jetwing becomes -1.72 and -1.75 for the leading-edge slat and droop configurations, respectively. All of these maximum horizontal tail lift coefficients occur at an uncorrected blowing coefficient of 0.96 and a flap deflection of 45 degrees [2].

Table 6 summarizes the stall angles of attack for each modification, elevator deflection. This table also gives estimated results for the actual horizontal tail of the Jetwing, based upon a graphical Reynolds number correction of 0.33 change in stall angle for a 1 x 10^6 change in Reynolds number [4]. The average Reynolds number used for the model application is 1 x 10^5 (based on an average tunnel speed of 25 ft/sec). The average Reynolds number for the actual Jetwing horizontal tail is 3 x 10^6 (based on a tail stall speed of 50 knots).

By extrapolating Figures 25-27 for the same Reynolds number effects, the maximum lift coefficients obtained for the slat and droop modifications to the actual horizontal tail become -2.03 and -1.71, respectively. This extrapolation is based on an average lift coefficient change of 0.05 per 1 x 10^6 change in lift coefficient [4].

Thus, it is obvious that both the leading-edge slat and droop modifications improve the stall characteristics of the Jetwing horizontal tail dramatically. However, from Figure 28, one can see that the leading-edge droop modification is the more drag efficient of the two proposed.

Static Longitudinal Stability

Although both modifications do improve the Jetwing's tail stall dramatically, both the slat and droop arrangements will probably affect the aircraft's static longitudinal instability very little. This observation arises form the fact that both the slat and droop configurations provide little chord, and thus area, increase. This small area increase results in a small change in the Jetwing's horizontal

Table 6. Summary of Flow Visualization Tests

Modification	Elevator (deg)	Model Stall Angle (deg)	Projected Tail Stall Angle (deg)*
None	0	-15	-16
None	10	-13	-14
None	20	-12	-13
None	30	-10	-11
Leading-Edge Slat	0	-28	-29
Leading-Edge Slat	10	-25	-26
Leading-Edge Slat	20	-23	-24
Leading-Edge Slat	30	-20	-21
Leading-Edge Droop	0	-23	-24
Leading-Edge Droop	10	-20	-21
Leading-Edge Droop	20	-19	-20
Leading-Edge Droop	30	-18	-19

*Based upon Reynolds number extrapolation

tail volume coefficient, as one can see from Table 7. Therefore, in order to increase the Jetwing's static longitudinal stability characteristics, a much larger chord extension device should be used.

Table 7. Horizontal Tail Volume Coefficient Comparison of Proposed Modifications

Modification	Horizontal Tail Volume Coefficient
None	0.750
Leading-Edge Droop	0.755
Leading-Edge Slat	0.761

CHAPTER VII

CONCLUSIONS AND RECOMMENDATIONS

The following conclusions and recommendations can be derived as a result of this research:

1. Both the leading-edge slat and droop modifications extend the stall capabilities of the Jetwing horizontal tail to larger angles of attack. However, the droop arrangement does not reach or exceed the maximum angle of attack derived from Kimberlin's [10] method.
2. While the leading-edge droop configuration stalls at a lower angle of attack, this configuration is probably more drag efficient due to its smaller size. In addition, the droop configuration would probably be much easier to manufacture than the slat.
3. Both modifications do contribute to the tail's contribution to static longitudinal stability; however, these improvements are quite small, and can almost be deemed negligible.

From these conclusions, the following recommendations can be drawn:

1. A full-scale flight-test investigation should be conducted with both the leading-edge slat and droop configurations applied to the horizontal tail of the Jetwing. Both static longitudinal stability and tail stall characteristics should

be examined during these tests. In addition, takeoff and landing tests should be conducted to determine the performance increase these modifications yield.

2. Larger slat and droop modifications should be designed and tested to determine if the aircraft's stability can be further improved.

BIBLIOGRAPHY

BIBLIOGRAPHY

1. Kimberlin, R., A. K. Sinha, and U. P. Solies, "A Flight Test Evaluation and Analytical Study of the Ball-Bartoe Jetwing Propulsive Lift Concept without Ejector," UTSI Report 82/17, The University of Tennessee Space Institute, Tullahoma, Tennessee, October 1, 1982.

2. Solies, U. P., "A Study of the Flow Field About an Upper Surface Blown Wing and Its Effects on Longitudinal Static Stability of a Small Jet Airplane," Thesis (Ph.D), The University of Tennessee, Knoxville, Tennessee, December 1985.

3. Kimberlin, R. D., "A Flight Test Evaluation of the Ball-Bartoe Jetwing Propulsive Lift Concept," UTSI Report 81-1, The University of Tennessee Space Institute, Tullahoma, Tennessee, July 1, 1981.

4. Abbott, Ira and Albert Von Doenhoff, Theory of Wing Sections. New York: Dover Publications, Inc., 1959.

5. McCormick, Barnes, Jr., Aerodynamics, Aeronautics, and Flight Mechanics. New York: John Wiley and Sons, Inc., 1949.

6. Hage, Robert and Courtland, Perkins, Airplane Performance Stability and Control. New York: John Wiley and Sons, Inc., 1949.

7. Nicolai, Leland, Fundamentals of Aircraft Design. San Jose, CA: METS, Inc., 1975.

8. Kimberlin, R. D., "A Conceptual Design Method for Upper Surface Blowing Aircraft," Unpublished Dissertation (Ph.D), 1989.

9. Ball-Bartoe Jetwing Wind-Tunnel Data, UTSI Flight Research Laboratory, Tullahoma, Tennessee, 1978.

10. "Airworthiness Standards: Normal, Utility and Aerobatic Category Airplanes," Federal Aviation Regulations, Part 23, Section 171, Washington, D. C., The United States Government Press, 1989.

11. Harper, John, "Wind-Tunnel Investigation of Effects of Various Aerodynamic Balance Shapes and Sweepback on Control Surface Characteristics of Semispan Tail Surfaces with NACA 0009, 0015, 66-009, 66(215)-014, and Circular-Arc Airfoil Sections," NACA Technical Note 2495, October 1951.

12. Sisterman, Steven, "A Proposed Solution to the Longitudinal Instabilities of the Ball-Bartoe Jetwing Through the Addition of a Thin, Fixed Slat to the Horizontal Tail," Thesis (M. S.), The University of Tennessee, Knoxville, Tennessee, May 1984.

13. DiCarlo, D., J. Patton, and A. Stough, "Flight Investigation of Stall, Spin, and Recovery Characteristics of a Low-Wing, Single-Engine, T-Tail Light Airplane," NASA Technical Paper 2427, May 1985.

14. UTSI Low-Speed Wind-Tunnel, Unpublished Information, UTSI Archives, The University of Tennessee Space Institute, Tullahoma, Tennessee.

15. Tietz, Thomas, "Experimental Investigation of Flexible Wings," Thesis (M. S.), The University of Tennessee, Knoxville, Tennessee, March 1986.

VITA

After graduating from Maryville High School, Maryville, Tennessee, in 1985, Mark McBride entered the University of Tennessee, Knoxville. In June 1987, he graduated with a Bachelor of Science Degree in Aerospace Engineering.

In January 1988, the author enrolled at The University of Tennessee Space Institute as a student and Graduate Research Assistant in the Flight Research Department of the Space Institute. In August 1989, he graduated from the University with a Master of Science Degree in Aviation Systems, with a concentration in the field of Flight Test Engineering.

The author is a member of the American Institute of Aeronautics and Astronautics and the Society of Flight Test Engineers. He is currently employed with McDonnell Aircraft Company in St. Louis, Missouri, as a Flight Test Engineer.